Available online at www.sciencedirect.com
SCIENCE DIRECT®
ELSEVIER
Nuclear Physics A 717 (2003) 149–198
NUCLEAR PHYSICS A
www.elsevier.com/locate/npe

Nuclear structure of ^{131}Te studied with (n, γ) and $(\vec{d}, p)$ reactions

I. Tomandl [a,*], T. von Egidy [b], J. Honzátko [a], V. Bondarenko [c], H.-F. Wirth [b], D. Bucurescu [d], V.Y. Ponomarev [e,f], G. Graw [g], R. Hertenberger [g], Y. Eisermann [g], S. Raman [h]

[a] *Nuclear Physics Institute, 250 68 Řež, Czech Republic*
[b] *Physik-Department, Technische Universität München, D-85748 Garching, Germany*
[c] *Institute of Solid State Physics, University of Latvia, Kengaraga 8, LV-1063 Riga, Latvia*
[d] *Horia Hulubei Institute of Physics and Nuclear Engineering, 76900 Bucharest, Romania*
[e] *Joint Institute for Nuclear Research, 141980 Dubna, Russia*
[f] *Institut für Kernphysik, Technische Universität Darmstadt, D-64289 Darmstadt, Germany*
[g] *Sektion Physik, Universität München, D-85748 Garching, Germany*
[h] *Oak Ridge National Laboratory, Oak Ridge, TN 37831, USA*

Received 24 September 2002; received in revised form 14 November 2002; accepted 18 November 2002

Abstract

The structure of ^{131}Te has been investigated with the ^{130}Te$(n, \gamma\gamma)^{131}$Te reaction using thermal neutrons and with the ^{130}Te$(d, p)^{131}$Te reaction using polarized deuterons with energy $E_d =$ 18 MeV. About 290 levels were identified in most cases including spin, parity and γ-decay. The γ-decay scheme after neutron capture is essentially complete containing about 100% of the decay of the capture state and about 100% of the population of the $11/2^-$ isomer and of the ground state. The scheme includes 42 primary transitions with energies between 750 keV and 2500 keV. The experimental level scheme is compared with predictions of the Interacting Boson–Fermion model (IBFM) and of the Quasiparticle Phonon Model (QPM). The isomeric ratio of the $11/2^-$ isomer at 182.31(5) keV was determined to be 0.054(2). The neutron binding energy is 5929.38(6) keV. The total thermal neutron capture cross section was found to be 186(13) mbarn.

PACS: 21.10.-k; 21.10.Jx; 21.60.Ev; 27.60.+j

Keywords: NUCLEAR REACTIONS ^{130}Te(n, γ), $E =$ thermal; measured E_γ, I_γ, $\gamma\gamma$-coincidence, binding energy; ^{130}Te(d, p), $E = 18$ MeV, polarized d; measured particle spectra, $\sigma(\theta)$, asymmetry; enriched targets;

* Corresponding author.
E-mail address: tomandl@ujf.cas.cz (I. Tomandl).

0375-9474/02/$ – see front matter
doi:10.1016/S0375-9474(02)01390-8

Ge detectors; magnetic spectrograph; ^{131}Te deduced levels, J^{π}, γ-branching ratios, DWBA, CCBA, spectroscopic factors, IBFM, QPM.

1. Introduction

The nuclear structure of tellurium isotopes ($Z = 52$) deserves special interest due to the vicinity to the magic tin nuclei with $Z = 50$. These isotopes are consequently an ideal tool for the investigation of the systematic evolution of various nuclear properties going from ^{119}Te, neutron midshell with $N = 67$, to ^{131}Te, $N = 79$, which approaches the doubly magic nucleus ^{132}Sn and also ^{134}Te, the most frequent fission fragment. There are several interesting questions which have to be solved in this region of the chart of nuclides. Which symmetry of the Interacting Boson Model (IBM) reproduces best these nuclei, U(5) or O(6) and are similar IBM parameters valid for all Te isotopes? Can we identify intruder states at low excitation energies? What is a mechanism of the strong $11/2^-$ isomer population in (γ, γ') and (n, γ) reactions? What is the role of direct neutron capture in the (n, γ) reaction on the Te isotopes? In addition, it is very important to establish the rather complete level schemes in long isotopic chains, like the Te one, to study the properties of many-body systems with increasing particle numbers. In order to give reliable and precise answers to these questions a large international collaboration investigates all Te isotopes which can be studied with (n, γ) and one-nucleon transfer reactions: ^{119}Te [1], ^{121}Te [2], ^{122}Te [3], ^{123}Te [4], ^{124}Te [5,6], ^{125}Te [7], ^{126}Te [8], ^{127}Te [9] and ^{129}Te [10].

The present publication reports new measurements of the ^{130}Te$(n, \gamma)^{131}$Te and ^{130}Te$(d, p)^{131}$Te reactions performed at Řež near Prague and at Garching near Munich, respectively. Previous experiments on ^{131}Te are compiled in the nuclear data dheets [11] and concern the (n, γ) reaction [12–14], the (d, p) reaction [15–17], the (t, d) reaction [18] and the β-decay of the fission fragment ^{131}Sb [19,20].

2. The (d, p) measurement

2.1. Experiment

The ^{130}Te$(d, p)^{131}$Te measurements were carried out using the polarized deuteron beam from the Tandem Accelerator of the University and Technical University of Munich. The spectra up to 3.2 MeV were measured at 18 MeV and 12 scattering angles from 11° to 70° with the Q3D spectrograph [21] and a 1.7 m long focal plane detector [22]. The energy resolution in the final proton spectra was between 4 to 5 keV. The 200 μg/cm^2 thick target was enriched in ^{130}Te (99.3%) and deposited on 4 μg/cm^2 carbon backing. Unfortunately there was a background of W lines in the spectra. However, these lines are easily identified due to the shift at different angles. The (d, p) spectrum at a scattering angle of 20° is shown up to 2.7 MeV in Fig. 1.

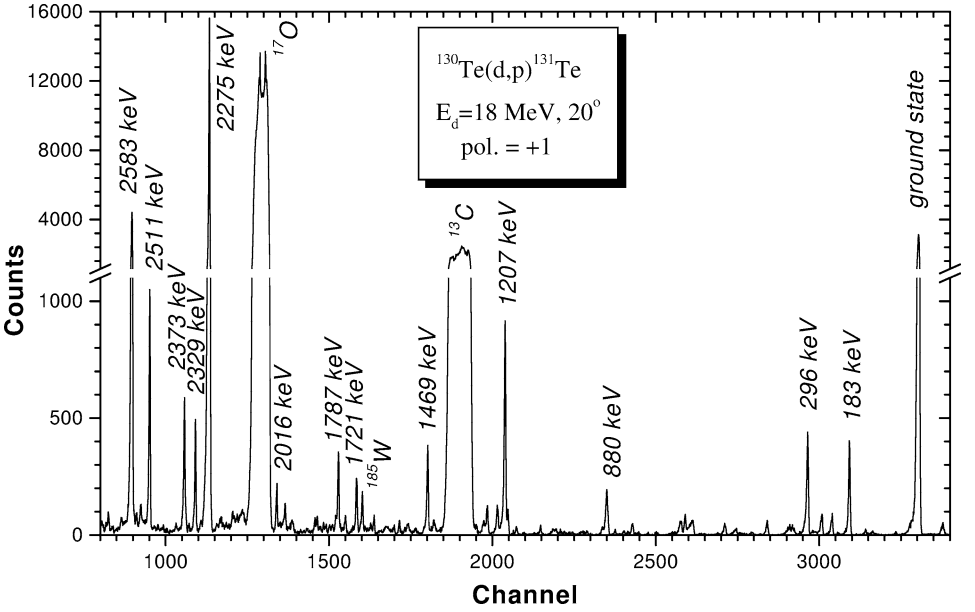

Fig. 1. The proton spectrum from the ^{130}Te$(d, p)^{131}$Te reaction measured at $E_d = 18$ MeV and scattering angle $\Theta_{\text{lab}} = 20°$.

Besides the angular distribution of the partial cross sections the asymmetries were analyzed for 11 scattering angles from 11° to 50°. The asymmetries were deduced from the equation

$$A_y = \frac{2}{3P_y}\frac{\sigma_+ - \sigma_-}{\sigma_+ + \sigma_-}, \tag{1}$$

where σ_+ and σ_- are measured differential cross sections with respect to the polarization of the beam and where P_y is the vector polarization. In our experiment, the value of the vector polarization amounts to 0.6. The angular distributions of the asymmetries enabled us to determine besides the transferred momentum l also definite spins for most of the levels observed in the measurement. Examples of the angular distributions of the cross sections and the asymmetries are shown in Fig. 2.

Preliminary results from the (d, p) measurement up to 3.2 MeV had shown a correlation between (d, p) and (n, γ) intensities. This correlation in ^{131}Te was firstly observed in Ref. [13] and can be explained within the framework of the direct capture mechanism in the ^{130}Te$(n, \gamma)^{131}$Te reaction which will be discussed in Section 7. This correlation motivated us to extend the (d, p) measurement up to 5.5 MeV with a new target. Additional runs of the (d, p) reaction at 7 scattering angles (from 11° to 30°) were performed within the energy range from 2.5 MeV to 5.5 MeV. To distinguish between two possible spins of the final level we used the polarized beam of deuterons at 3 scattering angles, namely 20°, 23° and 26°.

The energy calibration was done using level energies from the ^{130}Te$(n, \gamma)^{131}$Te measurements (see Section 3). Despite the precise level energies used for the calibration

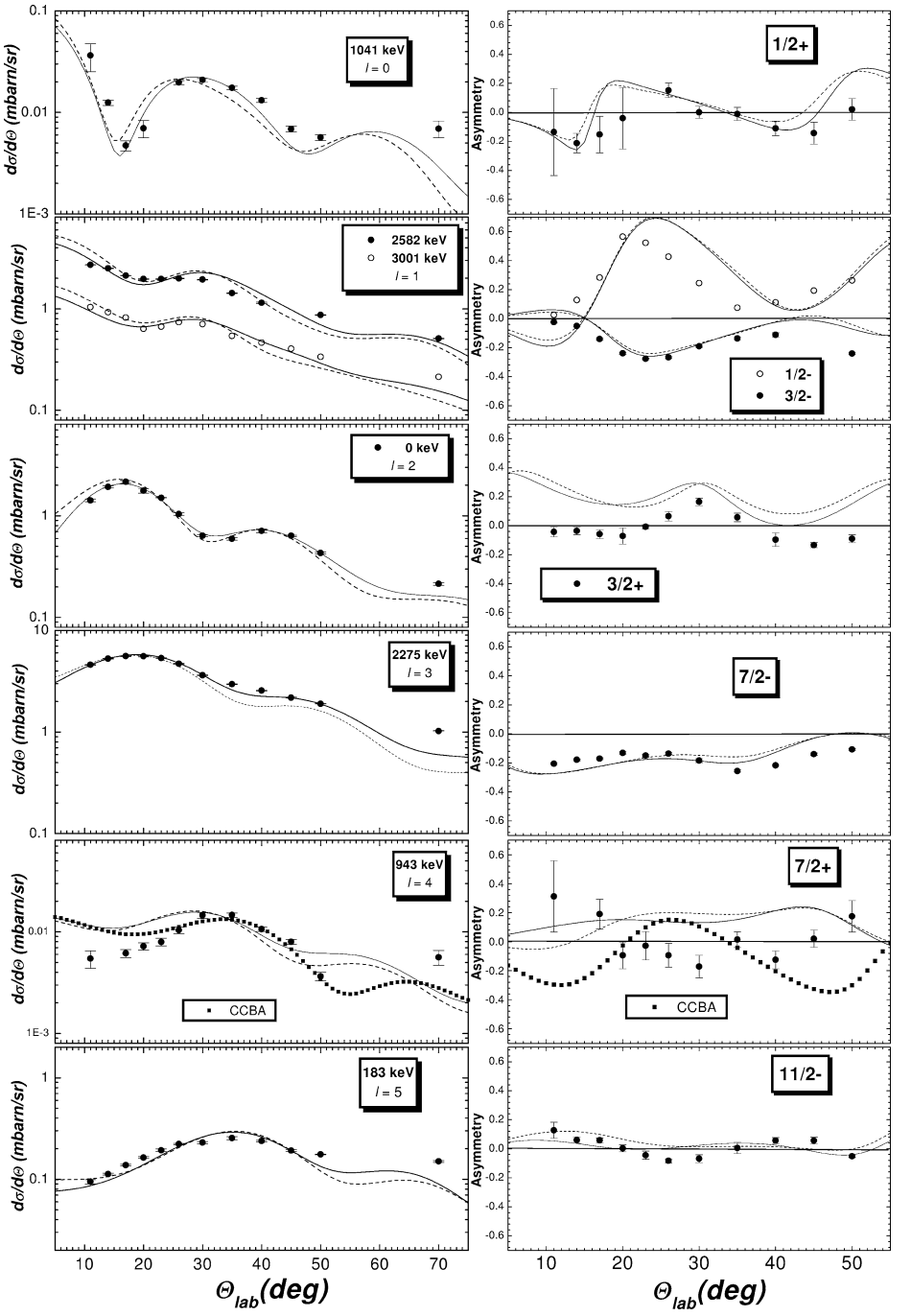

Fig. 2. DWBA fit of experimental partial cross sections and asymmetries. The dotted and solid curves are fits using the parameters of the optical potential A and B in Table 2, respectively.

and the excellent energy resolution in all transfer experiments with FWHM in the range from 3 keV to 5 keV, a systematic error of the level energies due to the local non-linear energy response of the detector about 0.5 keV should be added to statistical error given in the Table 1.

Using the integrated deuteron current of the Faraday cup, which was placed behind the target in the direction of the beam from the accelerator, we calculated absolute partial cross sections. The absolute partial cross sections at the scattering angle 20° are given in the Table 1.

2.2. DWBA and CCBA analysis

The experimental angular distributions of partial cross sections and asymmetries were compared with the theoretical prediction calculated by the coupled-channel code CHUCK3 [23]. The optical model parameters used in the analysis are given in Table 2. The proton parameters and the set A of the deuteron parameters were taken from the work of Strömich et al. [17]. For the calculation of the spectroscopic factors we employed the parameter set B [24] for the incoming channel which gave better agreement with the experimental distributions of the partial cross sections and asymmetries (see Fig. 2). The absolute values of the spectroscopic factors depend also on the bound neutron potential. While the neutron potential radius r_R was extracted from the recent evaluation of the neutron root mean square radii [25] the value of the diffuseness a_R was set equal to the appropriate proton value. The correction to the zero-range approximation was done by multiplying the radial form factor with the Hulthén function with the finite range parameter FNRG = 0.621. The nonlocality parameters nlc for the incoming and outgoing distorted waves and for the transferred particle bound state are also given in Table 2.

For most of the levels we assumed a direct reaction and a one-step stripping process. The spectroscopic factors of levels populated by the one-step stripping process were calculated using the relation

$$\frac{d\sigma^{\exp}}{d\theta} = S_{lj}\sigma_{lj}^{\mathrm{CHUCK3}}, \tag{2}$$

where the experimental cross sections $\frac{d\sigma^{\exp}}{d\theta}$ are fitted with the theoretical DWBA single particle cross sections $\sigma_{lj}^{\mathrm{CHUCK3}}$. Two-step processes were taken in account for some levels with small cross sections to improve the agreement with the experimental data. In the Coupled Channel Born Aproximation (CCBA) quadrupole excitation of the target and the final nucleus was allowed. In both cases we used the deformation parameter $\beta_2 = 0.10$ following from the experimental value of $B(\mathrm{E2}; 2^+ \to 0^+)$ in ^{130}Te. To calculate the spectroscopic factors of these levels we fitted the experimental cross sections as well as the asymmetries with a coherent sum of the one-step and two-step processes. The multi-step mechanism can significantly contribute to the final cross section mainly for $5/2^+$ and $7/2^+$ states as $2d_{5/2}$ and $1g_{7/2}$ orbits are too low below the Fermi level to be empty. The example of the CCBA analysis for the level at 943 keV is given in Fig. 2. The IBFM calculation (see below) have shown that the dominant contributions of wave functions of this level is $|2^+ \otimes 2d_{3/2}\rangle 7/2^+$. Our new spin and parity assignments obtained from the angular distributions are also given in Table 1.

Table 1
Nuclear levels of ^{131}Te from the present (n,γ) and (d,p) measurements and the nuclear data sheets [11] and proposed energies and spin-parities

(n,γ)	(d,p)					Ref. [11]		Adopted	
Level energy (keV)	Level energy[a] (keV)	l_n	J^π	$d\sigma/d\theta$ 20° (μb/sr)	$S_{ln,j}$	Level energy (keV)	J^π	Level energy (keV)	J^π
	0	2	$3/2^+$	1767(86)	0.25	0.0	$3/2^+$	0.0	$3/2^+$
182.34(4)	183	5	$11/2^-$	163(4)	0.15	182.50(20)	$11/2^-$	182.34(4)	$11/2^-$
296.02(1)	296.8(3)	0	$1/2^+$	219(6)	0.13	295.92(12)	$1/2^+$	296.02(1)	$1/2^+$
642.32(1)	642.2(2)	2	$5/2^+$	32(2)	0.0023	642.28(8)	$(5/2)^+$	642.32(1)	$5/2^+$
						776.88(12)		776.88(12)?	
802.28(4)	802.5(7)			8(2)[k]				802.28(4)	$(9/2^-)$
854.40(2)	854.2(1)	2	$3/2^+$	6.1(6)	0.0008	857(5)	$1/2^+$	854.40(2)	$3/2^+$
880.39(4)	879.9(2)	3	$7/2^-$	82(4)	0.0062	882(4)	$5/2^-, 7/2^-$	880.39(4)	$7/2^-$
943.45(5)	942.9(2)	4	$(7/2)^+$	7.2(6)	< 0.0002	943.32(8)	$7/2^+$	943.41(5)	$7/2^+$
						1036.68(15)?			
1041.73(8)	1041.3(2)	0	$1/2^+$	7.0(13)	0.0040	1043(4)	$1/2^+$	1041.73(8)	$1/2^+$
1050.84(2)	1051.6(2)	(2)	$3/2^+$	12.4(10)	0.0017	1051.07(16)	$(3/2^-, 5/2, 7/2)$	1050.84(2)	$3/2^+$
1207.11(3)	1206.7(1)	2	$5/2^+$	371(4)	0.027	1207.39(9)	$(5/2)^+$	1207.514(3)	$5/2^+$
1267.44(20)	1267.2(3)	(4)	$(7/2^+, 9/2^+)$	29(2)[l]	0.016	1267.51(18)	$(5/2)^+$	1267.548(13)	$7/2^+$
1398.91(7)	1398.3(3)	(2)	$5/2^+$	13(2)[l]	0.0015	1398.91(20)	$(3/2^-, 5/2, 7/2)$	1398.91(7)	$5/2^+$
						1400(5)	$9/2^-, 11/2^-$	1400.(5)??	$9/2^-, 11/2^-$
						1467.12(20)?	$(7/2, 9/2)$	1467.12(20)??	$(7/2, 9/2)$
1469.66(9)	1469.3(1)	2	$5/2^+$	146(2)	0.0090	1470.31(20)	$(5/2)^+$	1469.79(11)	$5/2^+$
						1544.78(17)?	$(5/2, 7/2)$	1544.78(17)??	$(5/2, 7/2)$
	1600.9(5)[b]	(2)		6.8(9)	0.00085	1601.40(17)?		1601.40(17)	$(3/2^+)$
1659.49(7)	1659.0(2)	3	$7/2^-$	31.2(13)	0.0020	1659(4)	$3/2^+, 5/2^+$	1659.49(7)	$7/2^-$
1670.26(21)	1669.4(8)[c]			4.7(9)[m]		1669.62(13)		1669.79(11)	$5/2, 7/2^+$
1678.30(8)								1678.30(8)	$1/2, 3/2, 5/2^+$
1683.10(8)								1683.10(8)	$1/2, 3/2, 5/2^+$
1721.63(7)	1721.1(2)	3, 2	$7/2^-, 5/2^+$	72(4)	0.0035	1722.0(5)	$(5/2)^+$	1721.63(7)	$5/2^+ (7/2^-)$
1756.01(5)								1756.01(5)	$(5/2^-)$

(*continued on next page*)

Table 1 (*Continued*)

(n,γ)	(d,p)					Ref. [11]		Adopted	
Level energy (keV)	Level energy[a] (keV)	l_n	J^π	$d\sigma/d\theta$ 20° (μb/sr)	$S_{ln,j}$	Level energy (keV)	J^π	Level energy (keV)	J^π
1781.22(6)	1779.7(3)	1	$3/2^-$	8.2(11)	0.0010			1781.22(6)	$3/2^-$
1787.97(6)	1787.1(1)	3	$7/2^-$	139(4)	0.010	1786(4)	$5/2^-, 7/2^-$	1787.97(6)	$7/2^-$
	1841.9(2)	2(3)	$5/2^+(7/2^-)$	18(2)	0.0013	1840(5)	$5/2^-, 7/2^-$	1841.9(5)	$5/2^+(7/2^-)$
1852.51(61)	1852.7(6)[d]	4(5)	$9/2^+, (11/2^-)$	10.6(13)	0.0028			1852.51(61)	$9/2^+, (11/2^-)$
						1854.4(3)?		1854.4(3)??	
1855.79(7)								1855.79(7)	$1/2^+, 3/2$
1867.07(14)	1866.4(3)	3, 2	$7/2^-(5/2^+)$	26.4(15)	0.0018	1865(5)	$1/2^+$	1867.07(14)	$7/2^-(5/2^+)$
	1875.4(2)[e]			3.2(9)[n]				1875.4(5)	
	1916.6(2)[f]			2.3(4)[o]				1916.6(5)	
1951.61(8)								1951.61(8)	$1/2^+, 3/2$
2015.46(4)	2016.1(1)	2	$5/2^+$	70(4)	0.0045	2014(4)	$1/2^-, 3/2^-$	2015.46(4)	$5/2^+$
						2066.83(20)	$(7/2^+, 9/2^+)$	2066.83(20)	$(7/2^+, 9/2^+)$
2092.02(4)	2091.4(1)	1	$3/2^-$	24.1(13)[l]	0.0020	2092(4)	$3/2^-, 1/2^-$	2092.02(4)	$3/2^-$
	2147.5(3)	2	$3/2^+$	17(2)	0.0020	2145(5)		2147.5(6)	$3/2^+$
						2180.1(4)	(5/2, 7/2)	2180.1(4)	(5/2, 7/2)
						2226.13(20)	(5/2, 7/2, 9/2)	2226.13(20)	(5/2, 7/2, 9/2)
2231.08(6)								2231.08(6)	$1/2^+, 3/2, 5/2^+$
	2275.2(1)	3	$7/2^-$	5559(53)	0.31	2278(4)	$(7/2)^-$	2275.2(5)	$7/2^-$
2330.21(20)	2329.1(1)	3	$7/2^-$	165(4)	0.0093			2330.21(20)	$7/2^-$
						2335.59(22)	$5/2^-$	2355.59(22)	$5/2^-$
2373.86(40)	2372.6(1)	3	$7/2^-$	211(4)	0.012	2372(4)	$(5/2^-, 7/2^-)$	2373.86(40)	$7/2^-$
	2393.7(4)	(2)	$(3/2^+)$	7.8(15)[k]	0.0008			2393.7(6)	$(3/2^+)$
						2398.42(11)	(5/2, 7/2)	2398.42(11)	(5/2, 7/2)
2457.17(9)	2458.3(4)[h]	2	$3/2^+$	65.2(11)				2457.17(9)	$3/2^+$
2496.60(9)	2497.9(4)			11.8(15)[p]		2496.33(25)	$(5/2^+, 7/2^+)$	2496.60(9)	$5/2^+$
	2503.6(3)			10(2)[p]				2503.6(6)	
2512.00(3)	2511.2(1)	1	$3/2^-$	424(6)	0.036	2511.45(24)	$(3/2)^-$	2512.00(3)	$3/2^-$

(*continued on next page*)

Table 1 (*Continued*)

(n,γ)	(d,p)					Ref. [11]		Adopted	
Level energy (keV)	Level energy[a] (keV)	l_n	J^π	$d\sigma/d\theta$ 20° (μb/sr)	$S_{ln,j}$	Level energy (keV)	J^π	Level energy (keV)	J^π
2544.26(12)								2544.26(12)	$5/2^-, 7/2^+$
2547.71(9)	2547.6(2)	1	$3/2^-$	38(2)	0.0024			2547.71(9)	$3/2^-$
						2551.97(19)	$(5/2^+)$	2551.97(19)	$(5/2^+)$
2582.54(2)	2582.5(1)	1	$3/2^-$	1964(13)	0.17	2582.68(24)	$(3/2)^-$	2582.54(2)	$3/2^-$
						2598.9(3)	$(5/2^+, 7/2^+, 9/2^+)$	2598.9(3)	$(5/2^+, 7/2^+, 9/2^+)$
						2662.22(19)	$(5/2^+, 7/2^+)$	2662.22(19)	$(5/2^+, 7/2^+)$
2671.36(18)								2671.36(18)	$1/2, 3/2$
2706.32(7)	2705.8(1)	1	$3/2^-$	19(2)	0.0015	2703(5)		2706.32(7)	$3/2^-$
2754.25(7)	2753.6(2)	1	$3/2^-$	49(2)	0.0038	2752(5)	$1/2^-, 3/2^-$	2754.25(7)	$3/2^-$
	2780.2(2)	3	$7/2^-$	34(2)	0.0014	2784(5)		2780.2(5)	$7/2^-$
	2788.4(6)			15(2)[p]				2788.4(8)	
	2828.8(1)	3	$7/2^-$	48(2)	0.0022			2828.8(5)	$7/2^-$
2932.48(9)	2932.8(2)	1	$1/2^-$	21(1)[k]	0.0032	2931(5)		2932.48(9)	$1/2^-$
	2980.7(3)	(2)	$(3/2^+)$	16(2)[p]	0.0015			2980.7(6)	$(3/2^+)$
3001.96(3)	3001.8(9)	1	$1/2^-$	739(11)	0.13	3002.42(22)	$(1/2)^-$	3001.96(3)	$1/2^-$
	3028.3(4)	2(3)		12(2)[p]	0.0023*	3027(5)?		3028.3(6)	
	3054.1(2)	3	$7/2^-$	49(2)	0.0022	3059(5)		3054.1(5)	$7/2^-$
	3073.2(2)	3	$5/2^-$	123(2)	0.0093	3069(5)		3073.2(5)	$5/2^-$
	3082.8(3)	3	$7/2^-$	24(1)	0.0014			3082.8(6)	$7/2^-$
	3097.0(4)	3	$5/2^-$	16(1)	0.0011			3097.0(6)	$5/2^-$
	3123.7(10)			1.9(6)				3123.7(11)	
	3142.3(2)	3	$5/2^-$	333(4)	0.025	3141(5)	$(5/2^-, 7/2^-)$	3142.3(5)	$5/2^-$
3146.23(19)								3146.23(19)	$1/2, 3/2, 5/2^+$
3170.76(24)								3170.76(24)	$1/2, 3/2, 5/2^+$
	3184.7(3)	3	$5/2^-$	436(4)	0.030	3183(5)	$(5/2^-, 7/2^-)$	3184.7(8)	$5/2^-$
3186.70(17)								3186.70(17)	$1/2^+, 3/2, 5/2^+$
	3203.4(3)	5	$9/2^-$	35(2)	0.023	3203(5)?		3203.4(6)	$9/2^-$

(*continued on next page*)

Table 1 (*Continued*)

(n,γ)	(d,p)					Ref. [11]		Adopted	
Level energy (keV)	Level energy[a] (keV)	l_n	J^π	$d\sigma/d\theta$ 20° (μb/sr)	$S_{ln,j}$	Level energy (keV)	J^π	Level energy (keV)	J^π
	3209.2(3)	3	$7/2^-$	38(2)	0.0015			3209.2(6)	$7/2^-$
	3239.6(3)	5, 4	$9/2^-, 7/2^+$	10(1)	0.0075			3239.6(3)	$9/2^-, 7/2^+$
	3262.5(4)	3	$7/2^-$	33(1)	0.0023			3262.5(6)	$7/2^-$
	3274.5(3)			7.3(6)				3274.5(6)	
	3291.3(5)	3, 2	$7/2^-, 5/2^+$	6.6(4)	0.00026			3291.3(7)	$7/2^-, 5/2^+$
	3301.9(7)	2, 3	$5/2^+, 7/2^-$	4.0(5)	0.00013			3301.9(9)	$5/2^+, 7/2^-$
	3311.6(6)	3	$5/2^-$	3.9(5)	0.00022			3311.6(8)	$5/2^-$
	3322.4(4)	3	$7/2^-$	13(1)	0.00050			3322.4(6)	$7/2^-$
	3333.6(5)	$\geqslant 4$		3.4(6)	0.00025			3333.6(7)	
	3354.0(2)	3	$7/2^-$	291(3)	0.012	3353(5)	$(5/2^-, 7/2^-)$	3354.0(5)	$7/2^-$
	3375.6(7)	5, 4	$11/2^-, 9/2^+$	22(3)	0.0060			3375.6(9)	$11/2^-, 9/2^+$
	3379.2(4)	2	$(5/2^+)$	69(3)	0.0022	3377(5)		3379.2(6)	$(5/2^+)$
	3404.1(2)	3	$7/2^-$	117(3)	0.0050	3401(5)		3404.1(5)	$7/2^-$
	3417.2(4)	3	$7/2^-$	218(3)	0.0090	3412(5)		3417.2(6)	$7/2^-$
	3425.5(2)	3	$7/2^-$	29(2)	0.0012			3425.5(5)	$7/2^-$
	3437.8(1)	3(2)	$(5/2^-)$	4.1(8)[k]	0.00030			3437.8(5)	$(5/2^-)$
	3443.0(3)	3(2)	$7/2^-(5/2^+)$	9.4(9)	0.00035			3443.0(6)	$7/2^-(5/2^+)$
	3458.8(3)	3	$7/2^-$	92(3)	0.0030	3457(5)		3458.8(6)	$7/2^-$
	3469.2(2)	3	$5/2^-$	129(3)	0.0090	3469(5)		3469.2(5)	$7/2^-$
	3473.5(6)			27(6)				3773.5(8)	
	3506.4(3)	3	$5/2^-$	62(3)	0.0044	3505(5)		3506.4(6)	$5/2^-$
3507.48(9)								3507.48(9)	$1/2^-, 3/2, 5/2^+$
	3510.7(6)	3	$5/2^-$	19(3)	0.0014			3510.7(8)	$5/2^-$
	3518.1(1)	3	$5/2^-$	171(3)	0.011	3517(5)		3518.1(5)	$5/2^-$
	3534.2(3)	3	$7/2^-$	25(1)	0.0010			3534.2(6)	$7/2^-$
3546.87(11)	3547.0(1)	1	$3/2^-$	92(3)	0.0090	3543(5)		3546.87(11)	$3/2^-$
	3552.3(1)	4(5)	$7/2^+(9/2^-)$	312(4)	0.030			3552.3(5)	$7/2^-$

(*continued on next page*)

Table 1 (*Continued*)

(n,γ)	(d,p)					Ref. [11]		Adopted	
Level energy (keV)	Level energy[a] (keV)	l_n	J^π	$d\sigma/d\theta$ 20° (μb/sr)	$S_{ln,j}$	Level energy (keV)	J^π	Level energy (keV)	J^π
3568.27(5)	3568.6(1)	1	$3/2^-$	148(2)	0.013	3563(5)		3568.27(5)	$3/2^-$
	3580.1(1)	3	$7/2^-$	69(2)	0.0026			3580.1(5)	$7/2^-$
3601.66(11)	3602.1(1)	1	$3/2^-$	125(2)	0.012	3600(5)	$(1/2^-, 3/2^-)$	3601.66(11)	$3/2^-$
3623.72(7)	3623.8(1)	1	$3/2^-$	87(2)	0.0090	3621(5)	$(1/2^-, 3/2^-)$	3623.72(7)	$3/2^-$
	3630.6(8)	(3)	$(5/2^-)$	10(1)	0.0007			3630.6(9)	$(5/2^-)$
	3640.9(7)[i]	3, 2	$(7/2^-, 5/2^+)$	6.3(7)	0.0004			3640.9(9)	$(7/2^-, 5/2^+)$
	3664.1(2)	3, 2	$7/2^-(5/2^+)$	415(5)	0.016	3663(5)	$3/2^+, 5/2^+$	3664.1(5)	$7/2^-(5/2^+)$
3668.25(10)			(1/2, 3/2)					3668.25(10)	(1/2, 3/2)
	3668.7(3)	3, 2	$7/2^-, 5/2^+$	76(6)[k]	0.0033			3668.7(6)	$7/2^-, 5/2^+$
	3672.3(7)	3, 2	$7/2^-, 5/2^+$	108(4)	0.0040			3672.3(9)	$7/2^-, 5/2^+$
3689.79(7)	3689.6(1)	1	$1/2^-$	134(3)	0.025	3690.1(4)	$1/2^-, 3/2^-$	3689.79(7)	$1/2^-$
3698.27(6)	3698.3(1)	1	$3/2^-$	65(2)	0.0065			3698.27(6)	$3/2^-$
	3709.5(1)	3	$7/2^-$	650(6)	0.025	3706(5)	$(3/2^+, 5/2^+)$	3709.5(5)	$7/2^-$
	3728.1(9)			6(1)				3728.1(10)	
3737.84(11)			(1/2, 3/2)					3737.84(11)	(1/2, 3/2)
	3739.1(7)	3	$7/2^-$	54(2)	0.0022	3736(5)		3739.1(9)	$7/2^-$
	3750.7(2)	1	$3/2^-$	28(1)	0.0022			3750.7(5)	$3/2^-$
3763.41(15)	3762.9(4)	1	$3/2^-$	11(1)	0.0008			3763.41(15)	$3/2^-$
	3771.4(2)	3	$7/2^-$	41(2)	0.0016			3771.4(5)	$7/2^-$
	3776.7(3)			15(3)[m]				3776.7(6)	
	3803.2(7)	3	$5/2^-$	7.0(7)	0.00045			3803.2(8)	$5/2^-$
	3820.4(9)	2, 3	$5/2^+, 7/2^-$	21(1)	0.0006			3820.4(11)	$5/2^+, 7/2^-$
	3825.5(12)	(1)	$(1/2^-)$	2.5(9)[l]	0.0004			3825.5(13)	$(1/2^-)$
	3842.0(6)			2(1)[n]				3842.0(8)	
	3847.4(3)	3	$7/2^-$	24(1)	0.0010			3847.4(6)	
	3857.8(2)	3(2)	$7/2^-(5/2^+)$	14(1)	0.0006			3857.8(2)	$7/2^-(5/2^+)$
	3871.1(9)			1.1(6)				3871.1(11)	

(*continued on next page*)

Table 1 (*Continued*)

(n,γ)	(d,p)					Ref. [11]		Adopted	
Level energy (keV)	Level energy[a] (keV)	l_n	J^π	$d\sigma/d\theta$ 20° (μb/sr)	$S_{ln,j}$	Level energy (keV)	J^π	Level energy (keV)	J^π
	3877.4(4)			5.2(6)[l]				3877.4(6)	
	3889.8(10)	(3)	$(5/2^-)$	4.3(7)	0.0003			3889.8(11)	$(5/2^-)$
	3895.9(9)	3	$5/2^-$	6.2(8)	0.0004			3895.9(10)	$5/2^-$
	3904.9(4)	2(3)	$5/2^+(7/2^-)$	139(3)	0.0040	3902(5)		3904.9(6)	$5/2^+(7/2^-)$
	3920.2(8)	3, 2		13(5)[p]	0.0008			3920.2(9)	
	3922.6(10)	3, 2	$5/2^-, 3/2^+$	37(4)	0.0020	3920(5)		3922.6(11)	$5/2^-, 3/2^+$
	3934.6(2)	3	$7/2^-$	85(7)	0.0030			3934.6(5)	$7/2^-$
3938.59(7)	3938.3(2)	1	$3/2^-$	165(7)	0.017	3935(5)	$1/2^-, 3/2^-$	3938.59(7)	$3/2^-$
	3956.0(5)	2, 3	$5/2^+, 7/2^-$	34(2)	0.0010			3956.0(7)	$5/2^+, 7/2^-$
	3964.2(3)	2, 3	$3/2^+, 5/2^-$	213(3)	0.010	3960(5)		3964.2(6)	$3/2^+, 5/2^-$
	3978.7(9)			6(1)				3978.7(10)	
3987.01(22)	3986.6(3)	1	$3/2^-$	77(3)	0.019	3985(5)	$1/2^-, 3/2^-$	3987.01(22)	$3/2^-$
	3991.4(4)	2	$3/2^+$	55(4)	0.0025			3991.4(6)	$3/2^+$
	3996.4(6)[g]			14(3)[p]				3996.4(8)	
	3998.4(2)	(1)	$(3/2^-)$	9(1)	0.0008			3998.4(5)	$(3/2^-)$
	4005.8(2)	3	$7/2^-$	109(2)	0.0036			4005.8(5)	$7/2^-$
	4018.2(2)	3	$5/2^-$	97(3)	0.0053			4018.2(2)	$5/2^-$
	4023.6(3)	3, 2	$7/2^-, 5/2^+$	33(3)[k]	0.0012			4023.6(6)	$7/2^-, 5/2^+$
4028.37(13)						4028(5)	$1/2^-, 3/2^-$	4028.37(13)	$(3/2^-)$
	4028.5(3)	3	$5/2^-$	229(4)	0.013			4028.5(6)	$5/2^-$
4036.63(5)	4036.1(2)	1	$3/2^-$	175(4)	0.019			4036.63(5)	$3/2^-$
	4041.9(3)	3, 2	$7/2^-, 5/2^+$	41(3)	0.0012			4041.9(6)	$7/2^-, 5/2^+$
	4053.7(3)	3, 2	$7/2^-, 5/2^+$	19(2)	0.0006			4053.7(6)	$7/2^-, 5/2^+$
4061.18(18)	4060.3(4)	1	$1/2^-$	14(2)	0.0030			4061.18(18)	$1/2^-$
4070.40(6)	4070.1(3)	1	$3/2^-$	266(4)	0.027	4071.1(3)	$1/2^-, 3/2^-$	4070.40(6)	$3/2^-$
	4073.8(10)	(1)	$(1/2^-)$	19(5)	0.0038			4073.8(11)	$(1/2^-)$
	4093.4(5)	3	$5/2^-$	119(3)	0.0066	4092(5)		4093.4(7)	$5/2^-$

(*continued on next page*)

Table 1 (*Continued*)

(n,γ)	(d,p)					Ref. [11]		Adopted	
Level energy (keV)	Level energy[a] (keV)	l_n	J^π	$d\sigma/s\theta$ 20° (μb/sr)	$S_{ln,j}$	Level energy (keV)	J^π	Level energy (keV)	J^π
4109.00(8)	4108.5(5)	1	$3/2^-$	55(4)[p]	0.0065	4107(5)		4109.00(8)	$3/2^-$
	4115.3(9)			7(2)				4115.3(10)	
4124.33(19)	4124.7(4)	1	$3/2^-$	34(2)	0.0036	4123(5)		4124.33(19)	$3/2^-$
	4136.2(2)	3	$5/2^-$	172(4)	0.0093	4135(5)		4136.2(5)	$5/2^-$
	4150.0(7)			7(1)				4150.0(9)	
	4157.4(2)	3	$5/2^-$	128(3)	0.0068	4155(5)		4157.4(5)	$5/2^-$
	4163.2(6)	3	$7/2^-$	21(3)[k]	0.0007			4163.2(8)	$7/2^-$
	4168.7(4)	6	$13/2^+$	37(2)	0.028			4168.7(6)	$13/2^+$
	4175.9(3)	5	$11/2^-$	72(3)	0.018	4175(5)		4175.9(6)	$11/2^-$
	4186.8(3)	4	$9/2^+$	77(3)	0.0032	4187(5)		4186.8(6)	$9/2^+$
	4191.8(5)	4	$9/2^+$	36(3)[k]	0.0020			4191.8(7)	$9/2^+$
	4196.2(11)	2	$5/2^+$	44(2)	0.0008			4196.2(12)	$5/2^+$
	4205.1(3)	4	$9/2^+$	116(3)	0.0060	4202(5)		4205.1(6)	$9/2^+$
	4211.7(2)	6	$13/2^+$	83(3)	0.060			4211.7(5)	$13/2^+$
	4225.1(7)	4	$7/2^+$	29(2)	0.0024			4225.1(9)	$7/2^+$
4238.98(15)	4239.3(3)	1	$1/2^-$	82(3)	0.016	4237(5)		4238.98(15)	$1/2^-$
	4246.0(2)	4	$9/2^+$	36(2)	0.0020			4246.0(5)	$9/2^+$
4253.59(6)	4252.8(3)	1	$1/2^-$	101(3)	0.020	4249(5)		4253.59(6)	$1/2^-$
	4260.5(3)	3	$7/2^-$	39(3)	0.0013			4260.5(6)	$7/2^-$
	4265.6(4)	3	$5/2^-$	24(2)	0.0013			4265.6(6)	$5/2^-$
	4272.3(6)			14(2)				4272.3(8)	
4278.62(15)	4277.7(3)	1	$3/2^-$	48(3)	0.0050			4278.62(15)	$3/2^-$
4285.80(6)	4285.2(2)	1	$3/2^-$	224(5)	0.023	4286.3(3)	$1/2^-, 3/2^-$	4285.80(6)	$3/2^-$
	4293.2(5)	2	$3/2^+$	71(3)	0.0030			4293.2(7)	$3/2^+$
4300.28(6)	4299.3(2)	1	$3/2^-$	96(3)	0.010	4297(5)	$(1/2^-, 3/2^-)$	4300.28(6)	$3/2^-$
	4309.6(3)	2	$3/2^+$	15(2)	0.0007			4309.6(6)	$3/2^+$
4324.59(7)	4324.6(7)	1	$3/2^-$	114(3)	0.010	4323(5)	$1/2^-, 3/2^-$	4324.59(7)	$3/2^-$

(*continued on next page*)

Table 1 (*Continued*)

(n,γ)	(d,p)					Ref. [11]		Adopted	
Level energy (keV)	Level energy[a] (keV)	l_n	J^π	$d\sigma/d\theta$ 20° (μb/sr)	$S_{ln,j}$	Level energy (keV)	J^π	Level energy (keV)	J^π
	4327.3(8)[g]			23(5)[l]				4327.3(10)?	
	4341.3(5)	3	$7/2^-$	85(7)	0.0030	4341(5)		4341.3(7)	$7/2^-$
	4344.6(2)	(1)	$(3/2^-)$	76(7)	0.0075			4344.6(5)	$(3/2^-)$
	4354.6(1)[g]			12(3)				4354.6(5)?	
	4358.0(7)	2	$3/2^+(5/2^+)$	45(3)	0.0013			4358.0(9)	$3/2^+(5/2^+)$
	4363.1(5)	3	$7/2^-$	108(4)	0.0036	4361(5)		4363.1(7)	$7/2^-$
4364.65(8)								4364.65(8)	$3/2^-$
	4373.1(7)	4	$9/2^+$	11(1)	0.0005			4373.1(9)	$9/2^+$
	4379.7(5)	3	$7/2^-$	14(4)	0.0005			4379.7(7)	$7/2^-$
	4383.5(6)	3	$7/2^-$	24(4)	0.0007			4383.5(8)	$7/2^-$
	4389.3(10)	(3)	$(7/2^-)$	21(2)	0.0006			4389.3(11)	$(7/2^-)$
	4393.1(7)[g]			14(4)				4393.1(9)?	
	4403.7(5)	3	$7/2^-$	9(1)	0.0003			4403.7(7)	$7/2^-$
	4412.1(2)	3	$7/2^-$	34(2)	0.0011			4412.1(5)	$7/2^-$
4425.07(12)	4426.1(3)	2	$3/2^+, 5/2^+$	51(2)	0.0025			4425.07(12)	$3/2^+(5/2^+)$
4436.83(34)	4437.3(3)	1	$3/2^-$	61(2)	0.0070			4436.83(34)	$3/2^-$
4445.79(24)	4445.4(3)	1	$3/2^-$	99(3)	0.011	4440(5)	$(1/2^-, 3/2^-)$	4445.79(24)	$3/2^-$
4453.80(36)	4453.1(3)	1	$1/2^-$	35(2)	0.0080			4453.80(36)	$1/2^-$
	4461.2(5)	2	$3/2^+$	39(2)	0.0019			4461.2(7)	$3/2^+$
	4472.1(3)	3	$7/2^-$	71(3)	0.0026	4471(5)		4472.1(6)	$7/2^-$
4472.57(10)								4472.57(10)	$3/2^-$
4485.25(14)	4485.2(7)	(1)	$(3/2^-)$	25(2)[k]	0.0025			4485.25(14)	$3/2^-$
4489.51(20)								4489.51(20)	$(1/2, 3/2)$
	4490.5(7)	4	$7/2^+$	140(4)[k]	0.0010	4487(5)		4490.5(8)	$7/2^+$
	4506.2(6)	2	$5/2^+$	108(6)[k]	0.0035			4506.2(8)	$5/2^+$
	4514.6(11)	1	$1/2^-, 3/2^-$	19(4)[p]	0.0060			4514.6(12)	$1/2^-, 3/2^-$
4519.98(9)								4519.98(9)	(3/2)

(*continued on next page*)

Table 1 (*Continued*)

(n,γ)	(d,p)					Ref. [11]		Adopted	
Level energy (keV)	Level energy[a] (keV)	l_n	J^π	$d\sigma/d\theta$ 20° (μb/sr)	$S_{ln,j}$	Level energy (keV)	J^π	Level energy (keV)	J^π
	4521.6(8)	2	$3/2^+$	186(15)[k]	0.010	4519(5)		4521.6(10)	$3/2^+$
4531.44(10)	4532.5(3)	1	$1/2^-$	82(7)[k]	0.018	4530(5)		4531.44(10)	$1/2^-$
	4539.4(5)	3(2)	$5/2^-(3/2^+)$	49(5)[p]	0.0024			4539.4(7)	$5/2^-(3/2^+)$
4545.18(7)	4544.4(3)	1	$1/2^-$	302(9)[p]	0.080	4543(5)	$(1/2^+)$	4545.18(7)	$1/2^-$
4558.45(6)	4558.5(5)	1	$1/2^-$	147(7)[p]	0.036	4558(5)	$(1/2^+)$	4558.45(6)	$1/2^-$
4563.18(6)	4563.8(5)	1	$3/2^-$	145(8)	0.018			4563.18(6)	$3/2^-$
	4570.8(8)	1	$(3/2^-)$	36(4)[p]	0.0047			4570.8(10)	$(3/2^-)$
4583.14(12)	4581.8(4)	1	$3/2^-$	54(4)	0.0066	4583(5)	$(3/2^+,5/2^+)$	4583.14(12)	$3/2^-$
	4587.1(10)	1	$3/2^-$	14(3)	0.0025			4587.1(11)	$3/2^-$
	4597.9(7)	4	$9/2^+$	8(2)	0.0004			4597.9(9)	$9/2^+$
	4610.6(5)			42(8)[p]				4610.6(7)	
	4614.3(13)	4	$(9/2^+)$	66(8)[p]	0.0035			4614.3(14)	$(9/2^+)$
	4620.1(8)	3	$5/2^-$	299(5)	0.015	4615(5)	$(3/2^+,5/2^+)$	4620.1(9)	$5/2^-$
	4628.9(9)	1	$1/2^-,3/2^-$	28(4)[m]	0.0050			4628.9(10)	$1/2^-,3/2^-$
4645.36(6)	4645.5(3)	1	$3/2^-$	112(4)	0.012	4644(5)	$(1/2^-,5/2^-)$	4645.36(6)	$3/2^-$
4649.93(9)	4650.3(6)	1	$3/2^-$	36(3)	0.0050			4649.93(9)	$3/2^-$
	4654.5(4)	3(2)	$5/2^-(3/2^+)$	29(3)	0.0015			4654.5(6)	$5/2^-(3/2^+)$
	4659.2(4)	3	$5/2^-$	233(4)	0.012			4659.2(6)	$5/2^-$
	4671.9(3)	3	$5/2^-$	53(3)	0.0031			4671.9(6)	$5/2^-$
	4678.0(6)	2,3		33(4)		4676(5)		4678.0(8)	
	4682.5(3)	6,7	$13/2^+,15/2^-$	16(3)[k]	0.0080			4682.5(6)	$13/2^+,15/2^-$
	4694.4(3)	3	$5/2^-$	122(3)	0.0065			4694.4(6)	$5/2^-$
4707.46(19)	4707.3(3)	2	$5/2^+(3/2^+)$	91(3)	0.0030	4706(5)		4707.46(19)	$5/2^+(3/2^+)$
	4716.7(4)	3	$5/2^-$	45(2)	0.0022			4716.7(4)	$5/2^-$
	4723.4(6)	3	$7/2^-$	58(3)	0.0020			4723.4(6)	$7/2^-$
	4727.3(6)	3	$7/2^-$	38(3)	0.0013			4727.3(6)	$7/2^-$
4732.74(18)	4733.0(3)	1	$3/2^-$	55(3)	0.0065	4730(5)		4732.74(18)	$3/2^-$

(*continued on next page*)

Table 1 (*Continued*)

(n,γ)	(d,p)					Ref. [11]		Adopted	
Level energy (keV)	Level energy[a] (keV)	l_n	J^π	$d\sigma/d\theta$ 20° (μb/sr)	$S_{ln,j}$	Level energy (keV)	J^π	Level energy (keV)	J^π
	4738.2(3)	2	$5/2^+(3/2^+)$	27(2)	0.0009			4738.2(6)	$5/2^+(3/2^+)$
	4743.7(6)	(3)	$(5/2^-)$	47(2)	0.0025			4743.7(8)	$(5/2^-)$
	4749.1(6)	(2, 3)		36(2)				4749.1(8)	
	4753.9(8)[e]			12(2)				4753.9(10)??	
	4756.0(4)[g]			12(3)				4756.0(6)?	
	4759.9(7)	3	$5/2^-$	27(2)	0.0013			4759.9(9)	$5/2^-$
	4765.6(2)	3	$7/2^-$	64(3)	0.0019	4763(5)		4765.6(5)	$7/2^-$
	4770.8(6)			29(3)				4770.8(8)	
	4775.2(9)			10(3)				4775.2(10)	
	4783.9(6)			8(1)				4783.9(8)	
	4789.8(5)	3	$7/2^-$	9(1)	0.0004			4789.8(7)	$7/2^-$
4801.23(12)								4801.23(12)	(3/2)
	4801.6(6)	3	$5/2^-$	42(2)	0.0020	4801(5)		4801.6(8)	$5/2^-$
	4808.8(5)	(3)	$(7/2^-)$	7(1)	0.0003			4808.8(7)	$(7/2^-)$
	4814.2(7)	(2)	$(5/2^+)$	33(2)	0.0015			4814.2(8)	$(5/2^+)$
	4820.8(3)			25(2)				4820.8(6)	
	4826.5(3)	3	$7/2^-$	73(3)	0.0025	4823(5)		4826.5(6)	$7/2^-$
	4842.9(3)	3, 2	$5/2^-, 3/2^+$	106(4)	0.0050	4843(5)		4842.9(6)	$5/2^-, 3/2^+$
	4847.2(3)	(1)	$(3/2^-)$	25(2)[k]	0.0024			4847.2(6)	$(3/2^-)$
4856.13(29)	4856.1(2)	2	$(3/2^+)$	50(2)	0.0024			4856.13(29)	$(3/2^+)$
	4863.5(5)	1, 2	$1/2^-, 3/2^+$	24(2)	0.0065			4863.5(7)	$1/2^-, 3/2^+$
4869.68(10)	4869.3(3)	1	$1/2^-$	53(3)	0.015	4869(5)		4869.68(10)	$1/2^-$
	4880.3(9)			15(2)				4880.3(10)	
	4888.5(4)			8(3)[m]				4888.5(6)	
4894.05(16)	4894.8(2)	1	$3/2^-$	48(4)[k]	0.0060	4892(5)		4894.05(16)	$3/2^-$
	4899.2(5)	(1)	$(1/2^-)$	18(3)[m]	0.0045			4899.2(7)	$(1/2^-)$
	4904.8(7)[g]			21(4)				4904.8(9)?	

(*continued on next page*)

Table 1 (*Continued*)

(n,γ)	(d,p)					Ref. [11]		Adopted	
Level energy (keV)	Level energy[a] (keV)	l_n	J^π	$d\sigma/d\theta$ 20° (μb/sr)	$S_{ln,j}$	Level energy (keV)	J^π	Level energy (keV)	J^π
	4907.3(7)	3, 2	$5/2^-, 3/2^+$	47(5)	0.0022			4907.3(9)	$5/2^-, 3/2^+$
	4911.9(7)	3, 2	$5/2^-, 3/2^+$	58(5)	0.0030			4911.9(9)	$5/2^-, 3/2^+$
	4914.8(13)	3	$7/2^-$	33(5)	0.0010			4914.8(14)	$7/2^-$
	4924.7(5)	2	$3/2^+$	11(2)	0.0005			4924.7(7)	$3/2^+$
	4929.9(4)	3	$5/2^-$	36(3)	0.0017			4929.9(6)	$5/2^-$
	4939.1(3)	3	$5/2^-$	111(5)	0.0055	4940(5)		4939.1(6)	$5/2^-$
4944.92(10)	4945.4(4)	1	$3/2^-$	32(3)	0.0045			4944.92(10)	$3/2^-$
	4958.7(6)	1	$1/2^-$	25(2)	0.0007			4958.7(8)	$1/2^-$
4964.21(14)	4964.5(5)	1	$3/2^-$	31(2)	0.0047	4964(5)		4964.21(14)	$3/2^-$
4970.36(11)	4970.7(5)	1	$3/2^-$	67(3)	0.0090			4970.36(11)	$3/2^-$
	4977.0(4)	(1)	$(1/2^-)$	85(3)	0.024			4977.0(6)	$(1/2^-)$
	4984.2(6)[g]			9(2)[k]				4984.2(8)?	
	4989.0(2)	(1)	$(1/2^-)$	52(2)	0.014			4989.0(5)	$(1/2^-)$
	4997.2(4)			37(3)		4998(5)		4997.2(6)	
	5000.8(3)			23(3)				5000.8(6)	
	5008.6(4)	$\geqslant 4$		18(2)				5008.6(6)	
	5012.7(5)	3	$5/2^-$	62(3)	0.0028			5012.7(7)	$5/2^-$
	5019.2(8)	6, 7	$13/2^+, 15/2^-$	15(2)	0.0090			5019.2(9)	$13/2^+, 15/2^-$
	5027.6(2)	6, 7	$13/2^+, 15/2^-$	24(2)	0.013	5027(5)		5027.6(5)	$13/2^+, 15/2^-$
	5034.5(3)	3	$5/2^-$	68(3)	0.0030			5034.5(6)	$5/2^-$
	5040.5(9)			15(2)				5040.5(10)	
5048.55(15)	5049.3(6)			37(2)		5049(5)		5048.55(15)	
	5056.4(4)	4	$7/2^+$	33(2)	0.0021			5056.4(6)	$7/2^+$
	5062.4(4)	(3)	$(5/2^-)$	53(2)	0.0025			5062.4(6)	$(5/2^-)$
	5074.6(12)			8(2)				5074.6(13)	
	5088.3(6)			29(1)[k]				5088.3(8)	
	5096.1(2)			9(1)[k]				5096.1(5)	

(*continued on next page*)

Table 1 (*Continued*)

(n,γ)	(d,p)					Ref. [11]		Adopted	
Level energy (keV)	Level energy[a] (keV)	l_n	J^π	$d\sigma/d\theta$ 20° (μb/sr)	$S_{ln,j}$	Level energy (keV)	J^π	Level energy (keV)	J^π
	5104.0(2)			82(3)[k]		5103(5)		5104.0(6)	
	5116.2(3)			31(2)[k]				5116.2(6)	
	5122.4(6)			39(2)[k]		5121(5)		5122.4(8)	
	5129.0(6)			39(2)[k]				5129.0(8)	
	5140.0(7)[e]			4(8)[k]				5140.0(9)??	
	5148.0(5)			78(14)[p]		5147(5)		5148.0(7)	
	5156.6(5)			56(9)[p]				5156.6(7)	
	5161.4(3)			56(8)[p]				5161.4(6)	
5172.23(25)	5172.3(7)			91(20)[p]				5172.23(25)	
	5177.1(8)			61(9)[p]				5177.1(10)	
	5183.0(8)[g]			56(8)[p]				5183.0(10)?	
	5191.3(13)			27(5)				5191.3(14)	
	5195.0(7)			64(7)				5195.0(9)	
	5203.2(10)			26(3)				5203.2(11)	

[*] $(2J+1)S_{dp}$.

[a] Only statistical errors are given. The systematic error of 0.5 keV has to be added in quadrature.

[b] Tentative level. Observed only at scattering angles 17°, 20° and 23°.

[c] Tentative level. Observed only at scattering angles 11° and 14°.

[d] Interference with the low-spin level at 1855.8 keV.

[e] Very tentative level.

[f] Tentative level. Observed only at scattering angles 45°, 50° and 70°.

[g] Tentative level.

[h] While partial cross section distribution prefers $l_n = 1$ the distribution of asymmetries is in agreement with a $3/2^+$ assignment.

[i] Small contribution from the ^{128}Te(d,p) ^{129}Te reaction.

[k,l,m,n,o,p] Partial cross section at scattering angles 23°, 26°, 14°, 40°, 45°, 17°, respectively.

Table 2
Set of parameters of optical potential for deuteron used in the DWBA analysis

Set	V_R (MeV)	$4W_D$ (MeV)	V_S (MeV)	r_R (fm)	r_I (fm)	r_S (fm)	r_C (fm)	a_R (fm)	a_I (fm)	a_S (fm)	nlc
					Deuteron parameters						
A	117.4	48.8	7.8	1.16	1.35	1.16	1.20	0.84	0.73	0.84	0.54
B	80.39	84.9	7.8	1.16	1.35	1.16	1.20	0.84	0.73	0.84	0.54
					Proton parameters						
	$63.0 - \frac{E_p}{2}$	44.0	7.5	1.22	1.23	1.22	1.25	0.67	0.67	0.67	0.85
					Bound neutron parameters						
	[a]		$\lambda = 25$	1.25				0.67			0.85

[a] Adjusted by the computer program to fit the neutron separation energy.

The high quality of the angular distributions of the partial cross section as well as the asymmetry in the whole range of measured excitation energies enables us to assign firmly spins and parities for most of states with an excitation energies up to 5 MeV. The most difficult task was to distinguish between $l = 2$ and $l = 3$ transferred momentum. However, combining the experimental distribution of partial cross sections and asymmetries we could arrive at an unambiguous spin and parity assignments also for these states. Additionally, $l = 1$ assignments were confirmed by the observed correlation between the intensities of the (d, p) and (n, γ) reaction (see Section 7) .

3. The (n, γ) measurements

Single γ-ray and coincidence γ–γ spectra were taken with the HPGe detector coincidence facility installed at the LWR-15 reactor in Řež [26]. The target of about 2.5 g with the enrichment of 99.3% in ^{130}Te was irradiated with the thermal neutron beam from the neutron guide (10^6 n/(cm^2 s). The large amount of coincidences accumulated during a period of 5 weeks allowed us to create coincidence spectra for about 150 gating transitions. About 220 γ-lines were observed in the single spectrum and a total of 440 in the coincidence spectra. In addition to these coincidences to individual lines twelve sum-coincidence spectra were created, i.e., spectra where the energy sum of two transitions corresponds to the energy difference between the capture state and a given level. The relative efficiency and the energy calibration of the detectors was obtained with ^{36}Cl transitions present in the spectra [27]. Relative intensities of γ transitions were converted in absolute units utilizing lines from β decay of ^{131}Te in the single γ spectrum [11]. The intensities of transitions which were observed only in a coincidence spectrum were calculated using a line or lines from the same coincidence spectrum with known absolute intensity and neglecting γ–γ angular correlation. The list of all observed γ transition energies (γ energy without recoil correction) with absolute intensities and placements is given in Table 3. The systematic intensity error of 5% is not included in the table. Lines with intensities less than 0.07 per 100 c.n. (captured neutrons) or with intensity errors equal or larger than 50% have a probability of about 5–10% to be nonexistent. Many peaks in

Table 3
List of observed γ transitions with their absolute intensities and their placement

Transition (keV)	$I\ \frac{1}{100n}$	$\frac{\Delta I}{I}$ (%)	E_i (keV)	Transition (keV)	$I\ \frac{1}{100n}$	$\frac{\Delta I}{I}$ (%)	E_i (keV)
211.7(5)	0.23	50	854	799.6(8)	0.04	25	–
227.1(3)	0.02	50	2015	804.96(9)	0.22	13	1856
229.9(3)	0.07	50	1951	807.8(3)	0.12	15	2015
296.01(1)	47.66	1	296	813.3(4)	0.04	75	1856
310.9(3)	0.06	50	2092	815.0(8)	0.03	67	1670
324.3(3)	0.06	33	1268	823.85(18)	0.11	25	1678
332.2(7)	0.06	50	2015	828.59(8)	0.52	7	1683
335.9(3)	0.05	60	2092	829.2(6)	0.09	40	2512
352.5(8)	0.03	67	1207	837.06(21)	0.09	40	1781
355.89(5)	0.29	17	2015	853.2(5)	0.05	60	2512
408.49(1)	1.49	1	1051	854.39(2)	3.54	1	854
419.44(5)	0.46	4	3002	857.15(3)	0.56	8	1659
419.9(3)	0.04	50	2512	860.7(3)	0.08	33	2582
455.59(20)	0.09	50	1399	861.61(19)	0.09	30	3568
457.2(4)	0.05	40	1856	868.0(6)	0.14	40	3624
475.33(9)	0.14	13	2933	875.61(3)	0.46	12	1756
490.03(20)	0.15	29	3002	880.78(16)	0.14	13	–
496.5(3)	0.04	50	2512	900.85(3)	0.36	8	1781
490.74(24)	0.17	37	2582	900.9(3)	0.13	36	1951
515.0(5)	0.18	25	1722	907.57(5)	0.26	7	1788
525.87(17)	0.10	18	1470	909.97(20)	0.06	57	1951
544.3(5)	0.03	67	1399	910.59(20)	0.32	6	1207
545.8(5)	0.04	60	2015	917.52(13)	0.19	48	3624
547.31(18)	0.08	22	–	926.2(5)	0.05	40	1781
558.2(4)	0.37	20	854	929.35(11)	0.20	23	4531
567.07(5)	0.33	19	2582	943.44(4)	0.55	7	944
586.05(19)	0.07	25	–	950.5(3)	0.06	33	2706
616.4(5)	0.04	60	2015	953.71(15)	0.16	29	1756
619.8(3)	0.10	45	1670	959.02(10)	0.35	11	5929
619.93(2)	1.11	3	802	965.17(14)	0.17	17	–
625.23(22)	0.19	24	1268	984.46(10)	0.33	11	5929
632.03(19)	0.17	32	1683	985.65(11)	0.08	33	1788
636.80(17)	0.11	50	1678	986.73(17)	0.13	29	1867
642.28(2)	6.36	1	642	998.2(4)	0.05	40	2754
661.9(3)	0.13	21	2754	1000.9(4)	0.06	29	1856
670.29(12)	0.12	23	2330	1019.4(6)	0.14	53	3602
698.07(2)	3.82	2	880	1024.1(3)	0.06	43	2231
708.60(15)	0.08	56	2497	1035.29(11)	0.20	14	5929
726.84(20)	0.25	18	1670	1040.84(10)	0.92	50	1683
738.87(15)	0.31	12	2754	1041.5(7)	0.06	50	2092
739.4(3)	0.05	60	1781	1041.68(20)	2.77	17	1042
744.49(11)	0.21	17	1951	1050.2(6)	0.02	50	1852
754.89(4)	1.36	9	1051	1050.91(3)	1.97	1	1051
755.4(4)	0.05	40	2512	1059.73(7)	0.21	17	5929
756.7(3)	0.72	25	1399	1064.69(22)	0.06	33	1867
757.3(3)	0.14	67	5929	1071.7(3)	0.12	31	2754
779.28(12)	0.13	55	1659	1071.80(17)	0.09	40	3568
789.0(5)	0.04	50	1670	1073.1(3)	0.18	21	–
791.62(14)	0.19	19	2548	1075.99(7)	0.28	10	2754

(*continued on next page*)

Table 3 (*Continued*)

Transition (keV)	$I\ \frac{1}{100n}$	$\frac{\Delta I}{I}$ (%)	E_i (keV)	Transition (keV)	$I\ \frac{1}{100n}$	$\frac{\Delta I}{I}$ (%)	E_i (keV)
1079.58(16)	0.11	17	1722	1475.7(5)	0.11	58	5929
1097.4(3)	0.23	40	1951	1476.33(13)	0.09	30	3568
1112.84(9)	0.23	16	2582	1477.0(7)	0.22	38	1659
1128.14(12)	0.18	20	5929	1483.0(5)	0.09	60	4485
1135.13(5)	0.28	10	2015	1483.4(4)	0.46	54	5929
1151.07(8)	0.30	9	2933	1484.0(6)	0.09	50	4239
1159.2(5)	0.14	20	4708	1485.0(3)	0.51	45	1781
1161.8(5)	0.13	29	2015	1488.3(4)	0.06	33	4489
1170.9(4)	0.07	50	3187	1492.6(3)	0.09	20	–
1180.6(4)	0.10	18	2231	1492.9(10)	0.03	67	2374
1183.65(8)	0.30	6	2582	1496.78(16)	0.14	20	2548
1187.3(14)	0.07	38	2231	1504.32(10)	0.27	10	5929
1196.71(12)	0.42	11	5929	1505.3(6)	0.06	50	2548
1207.11(4)	1.76	3	1207	1515.6(10)	0.12	22	4028
1211.85(16)	0.23	16	2092	1524.5(3)	0.11	25	4279
1213.2(4)	0.06	29	1856	1528.04(16)	0.23	12	2330
1221.93(10)	0.19	15	5929	1531.66(6)	0.60	5	2582
1226.18(23)	0.11	25	3738	1532.3(5)	0.06	57	3624
1230.1(4)	0.09	43	2497	1540.5(7)	0.14	33	2582
1241.0(3)	0.08	23	3698	1542.84(17)	0.20	14	4545
1250.8(8)	0.05	40	2457	1556.52(18)	0.18	16	4558
1267.6(3)	0.13	14	1268	1564.73(8)	0.40	9	5929
1277.3(6)	0.12	54	2544	1571.6(4)	0.09	60	2374
1279.46(9)	0.30	15	5929	1582.9(3)	0.08	22	–
1284.03(4)	0.73	10	5929	1588.48(14)	0.21	13	2231
1292.7(3)	0.18	53	3624	1602.9(3)	0.29	16	2457
1302.13(18)	0.05	95	–	1604.81(7)	0.55	5	5929
1303.9(6)	0.06	50	2512	1608.27(22)	0.20	45	3624
1309.20(24)	0.10	27	1951	1615.9(3)	0.07	38	2497
1315.29(10)	0.19	14	–	1629.10(6)	0.58	5	5929
1346.22(12)	0.22	13	5929	1629.6(4)	0.06	71	2671
1359.34(16)	0.25	19	3690	1642.3(3)	0.20	23	2497
1366.20(6)	0.91	5	5929	1643.55(5)	1.37	3	5929
1370.95(5)	1.34	3	5929	1650.70(19)	0.36	15	5929
1375.1(10)	0.04	50	2582	1663.9(3)	0.19	48	2544
1382.1(5)	0.38	12	1678	1665.0(5)	0.09	50	2706
1384.22(5)	2.80	3	5929	1675.83(6)	0.90	7	5929
1397.95(10)	0.32	57	5929	1678.5(3)	0.13	50	1678
1399.0(3)	0.74	25	1399	1683.50(12)	1.23	8	1683
1405.4(10)	0.18	50	2457	1689.4(3)	0.25	19	2544
1405.7(4)	0.07	50	3187	1690.46(9)	1.10	5	5929
1409.42(8)	0.43	9	5929	1702.45(17)	0.40	5	2582
1414.3(15)	0.10	100	2457	1703.3(7)	0.09	40	2754
1440.3(3)	0.55	50	5929	1721.54(7)	0.76	5	1722
1444.12(14)	0.24	12	4446	1737.8(5)	0.08	45	3690
1450.8(5)	0.23	16	2330	1737.8(5)	0.08	45	4286
1456.80(10)	0.42	11	5929	1742.05(9)	0.15	38	2544
1459.7(9)	0.03	67	2512	1751.51(9)	0.28	10	3507
1469.77(23)	0.78	28	1470	1756.08(17)	0.12	23	1756
1470.2(3)	0.11	25	2512	1770.25(22)	0.14	40	–

(*continued on next page*)

Table 3 (*Continued*)

Transition (keV)	$I\ \frac{1}{100n}$	$\frac{\Delta I}{I}$ (%)	E_i (keV)	Transition (keV)	$I\ \frac{1}{100n}$	$\frac{\Delta I}{I}$ (%)	E_i (keV)
1780.89(12)	0.43	36	1781	2422.01(18)	0.34	8	5929
1795.94(6)	0.69	5	2092	2456.7(4)	0.59	5	2457
1800.9(4)	0.13	21	–	2472.5(4)	0.08	44	4254
1805.10(13)	0.29	10	4037	2495.4(3)	0.22	13	3547
1817.3(7)	0.12	31	2671	2504.7(3)	0.14	40	3547
1820.36(8)	0.57	6	5929	2512.05(6)	3.25	1	2512
1855.82(12)	0.42	9	1856	2530.6(8)	0.06	50	3738
1859.00(5)	1.73	2	5929	2544.3(6)	0.07	50	3187
1868.08(15)	0.26	21	5929	2546.6(5)	0.33	42	2548
1873.80(10)	0.34	11	2754	2548.26(21)	0.48	19	2548
1890.5(9)	0.15	50	2933	2549.7(5)	0.18	50	3602
1892.70(4)	1.50	2	5929	2556.3(6)	0.09	50	4239
1901.02(13)	0.39	10	5929	2581.8(4)	0.13	29	3624
1901.1(4)	0.08	33	2544	2582.58(6)	4.87	1	2582
1905.02(21)	0.18	26	2548	2599.7(7)	0.06	50	4070
1935.7(6)	0.03	67	2231	2617.6(6)	0.09	30	3668
1940.4(3)	0.37	38	2582	2623.0(3)	0.24	19	–
1942.4(4)	0.46	20	5929	2636.21(23)	0.12	23	2933
1951.05(9)	1.49	12	3002	2647.1(7)	0.10	45	3698
1951.3(4)	0.46	50	1951	2648.4(9)	0.07	50	3690
1960.1(4)	0.14	33	3002	2652.8(5)	0.09	50	3507
1990.78(7)	0.80	5	5929	2665.0(9)	0.18	35	3547
2015.9(3)	0.51	9	2015	2671.3(3)	0.18	50	2671
2092.10(10)	0.63	19	2092	2685.9(9)	0.01	100	3738
2097.1(7)	0.10	27	3568	2689.3(10)	0.07	50	3568
2144.1(3)	0.20	23	3187	2691.2(9)	0.04	75	3547
2147.50(20)	0.26	18	3002	2705.0(8)	0.09	60	4485
2161.2(7)	0.19	43	2457	2705.86(6)	7.18	1	3002
2162.2(9)	0.11	42	4254	2706.40(20)	0.10	36	2706
2165.96(14)	0.38	10	5929	2713.6(9)	0.09	50	3568
2191.63(13)	0.35	10	5929	2742.34(16)	0.32	12	5929
2200.56(15)	0.23	16	2497	2743.4(6)	0.11	33	3624
2209.3(5)	0.08	141	–	2746.1(7)	0.09	50	3602
2215.93(5)	4.51	3	2512	2754.0(4)	0.09	50	2754
2231.07(7)	0.46	100	5929	2758.5(3)	0.21	13	–
2231.07(7)	0.46	100	2231	2768.2(10)	0.04	50	3624
2239.64(6)	1.98	5	5929	2783.10(19)	0.23	12	5929
2251.5(8)	0.14	47	2548	2797.8(3)	0.21	22	–
2261.06(11)	0.55	12	5929	2828.7(12)	0.06	50	4037
2269.7(7)	0.05	40	3668	2830.6(8)	0.06	50	4300
2286.48(5)	26.77	1	2582	2863.13(20)	0.13	21	4070
2291.9(9)	0.06	57	3146	2903.0(13)	0.03	100	3547
2305.60(6)	1.14	2	5929	2925.64(18)	0.66	11	3568
2327.62(11)	1.41	4	5929	2927.0(3)	0.05	80	4708
2332.1(5)	0.07	50	3187	2927.33(6)	14.71	1	5929
2349.2(4)	0.15	38	4070	2932.8(4)	0.17	17	2933
2361.05(6)	1.77	2	5929	2959.28(22)	0.24	38	3602
2361.1(3)	0.25	19	3568	2996.59(10)	0.90	5	5929
2382.47(8)	1.04	3	5929	3001.87(6)	4.84	1	3002
2410.10(12)	0.45	8	2706	3019.9(5)	0.04	50	4070

(*continued on next page*)

Table 3 (*Continued*)

Transition (keV)	$I\ \frac{1}{100n}$	$\frac{\Delta I}{I}$ (%)	E_i (keV)	Transition (keV)	$I\ \frac{1}{100n}$	$\frac{\Delta I}{I}$ (%)	E_i (keV)
3025.9(6)	0.09	30	3668	3526.9(8)	0.14	67	4733
3030.1(6)	0.02	100	4070	3533.3(14)	0.04	50	4583
3055.1(13)	0.05	60	3698	3547.10(23)	0.41	11	3547
3058.8(13)	0.06	67	3938	3568.1(3)	0.25	15	3568
3093.9(5)	0.05	40	–	3571.4(7)	0.07	75	4425
3095.7(5)	0.05	40	3738	3590.2(10)	0.03	67	4473
3131.9(8)	0.09	40	3987	3592.3(9)	0.06	67	4473
3146.0(6)	0.05	80	3146	3602.0(3)	0.28	33	3602
3155.3(7)	0.23	16	4037	3623.3(5)	0.08	22	3624
3170.6(5)	0.11	67	3171	3635.6(5)	0.18	50	4279
3175.0(10)	0.08	44	4028	3642.43(17)	0.88	6	3938
3175.24(10)	1.17	5	5929	3643.6(8)	0.06	43	4286
3175.4(6)	0.05	40	4645	3658.5(5)	0.05	60	4300
3181.0(7)	0.10	36	4037	3667.80(24)	0.47	10	3668
3189.8(10)	0.12	31	4070	3682.4(4)	0.11	42	4325
3203.5(7)	0.06	43	4254	3683.5(7)	0.07	63	4563
3212.5(4)	0.09	30	4254	3689.99(10)	1.38	13	3690
3223.00(21)	1.01	18	5929	3690.9(4)	0.18	50	4545
3234.1(11)	0.06	50	4286	3691.1(4)	0.18	50	3987
3250.0(9)	0.04	75	4300	3698.15(13)	0.46	100	5929
3250.9(3)	0.06	33	3547	3698.15(13)	0.46	100	3698
3257.9(7)	0.06	50	4300	3732.4(8)	0.09	60	4028
3258.2(4)	0.15	36	5929	3737.7(13)	0.05	60	4945
3271.6(8)	0.06	43	3568	3740.40(14)	0.72	8	4037
3273.4(13)	0.05	60	4325	3759.4(5)	0.06	57	4801
3283.0(8)	0.11	42	4325	3762.8(11)	0.09	80	3763
3305.41(19)	0.33	8	3602	3774.47(11)	0.79	23	4070
3312.7(8)	0.04	50	4520	3791.5(12)	0.02	50	4645
3327.4(3)	0.67	12	3624	3812.2(5)	0.09	80	4109
3346.76(7)	32.03	1	5929	3831.0(20)	0.02	100	4473
3372.4(5)	0.09	30	3668	3837.27(19)	0.37	10	5929
3381.55(11)	0.75	6	5929	3912.6(5)	0.54	26	5929
3393.93(23)	0.07	50	4037	3921.5(6)	0.06	43	4563
3393.93(23)	0.17	22	3690	3938.81(24)	0.37	10	3938
3402.4(4)	0.17	28	3698	3944.0(5)	0.28	20	4239
3405.6(8)	0.06	67	4286	3957.65(23)	0.42	13	4254
3417.32(7)	7.82	1	5929	3978.2(4)	0.36	21	5929
3437.6(9)	0.06	33	4489	3981.7(6)	0.12	62	4279
3442.0(12)	0.01	100	3738	3986.9(4)	0.15	25	3987
3447.8(5)	0.10	18	4489	3989.60(11)	0.84	4	4286
3468.6(10)	0.09	80	3763	4004.3(4)	0.18	31	4300
3471.0(8)	0.37	25	5929	4028.6(8)	0.09	60	4028
3471.3(11)	0.11	67	4520	4028.8(3)	0.23	40	4325
3471.7(11)	0.06	57	4325	4036.2(3)	0.11	17	4037
3478.6(10)	0.15	63	4520	4060.7(3)	0.13	71	4061
3482.5(4)	0.06	57	4124	4065.0(10)	0.05	80	4708
3483.5(13)	0.02	50	4365	4069.0(5)	0.05	60	4365
3499.8(11)	0.03	67	4708	4070.4(4)	0.11	17	4070
3507.6(7)	0.14	67	3507	4073.4(3)	0.38	10	5929
3511.9(16)	0.04	50	4563	4092.2(10)	0.07	63	4733

(*continued on next page*)

Table 3 (*Continued*)

Transition (keV)	$I\ \frac{1}{100n}$	$\frac{\Delta I}{I}$ (%)	E_i (keV)	Transition (keV)	$I\ \frac{1}{100n}$	$\frac{\Delta I}{I}$ (%)	E_i (keV)
4109.1(3)	0.44	10	4109	4519.9(7)	0.13	71	4520
4148.0(10)	0.04	75	5929	4531.48(24)	0.42	9	4531
4149.4(4)	0.25	22	4446	4545.37(11)	1.54	3	4545
4157.7(7)	0.08	56	4454	4558.65(18)	0.82	6	4558
4176.3(5)	0.16	28	4473	4558.9(9)	0.06	71	4856
4193.5(3)	0.26	14	4489	4563.1(5)	0.17	22	4563
4207.3(3)	0.39	9	5929	4574.6(8)	0.07	50	4870
4224.5(8)	0.18	60	4520	4582.1(12)	0.02	100	4583
4239.9(5)	0.33	14	4239	4597.2(5)	0.20	18	4894
4246.5(4)	1.26	19	5929	4646.0(3)	0.35	13	4645
4249.5(7)	0.69	35	4545	4648.9(8)	0.08	56	4945
4253.5(3)	0.34	16	4254	4649.9(4)	0.04	75	4650
4267.0(3)	0.41	20	4563	4668.1(5)	0.09	60	4964
4278.9(14)	0.19	48	4279	4674.4(4)	0.12	38	4970
4286.9(4)	0.09	60	4583	4721.7(6)	0.12	38	5929
4287.1(6)	0.04	50	4286	4733.1(8)	0.14	67	4733
4324.9(20)	0.05	100	4970	4870.1(4)	0.35	13	4870
4349.4(3)	0.21	22	4645	4876.5(8)	0.10	36	5172
4354.0(4)	0.03	100	4650	4877.2(8)	0.14	40	5929
4364.2(14)	0.02	50	4365	4887.7(5)	0.30	31	5929
4445.8(5)	0.15	50	4446	5074.92(24)	0.66	8	5929
4489.2(6)	0.06	29	4489	5172.3(5)	0.14	67	5172

the single spectrum are multiplets and the intensities of the individual lines were obtained from the coincidence spectra.

The placement of the transitions was essentially based on the coincidence relations. The gamma decay of the levels is given in the Table 4. Although it is not explicitly stated, nearly all transitions are confirmed in their placement by corresponding coincidences. The depopulation of the capture state is (95.6 ± 1.0) per 100 c.n. (without the systematic error of 5 per 100 c.n.). The population of the $11/2^-$ isomer is (5.2 ± 0.1) per 100 c.n. The γ population of the ground state without isomeric transition is (96.2 ± 1.1) per 100 c.n. Consequently the total population of the ground and isomeric state is (103.3 ± 1.2) per 100 c.n. with additional systematic error of 5 per 100 c.n. Therefore, it can be stated that nearly 100% of the depopulating transitions of the capture state and nearly 100% of the ground and isomeric state population was observed. This completeness of an (n, γ) level scheme for a heavier nucleus is quite unusual.

With the populations of the ground state and of the $11/2^-$ isomer the isomeric ratio is calculated to be 0.054(2). Statistical decay of the $1/2^+$ capture state would predict a much smaller population of an $11/2^-$ level. The reason for the strong population was already discussed by us [4,28]. It is caused by the large mixing of the $11/2^-$ neutron wave function with quadrupole phonons and $3p$ and $2f$ components. This is confirmed by the theory. Consequently there are fast gamma cascades such as $1/2^+$ (capture state) $\rightarrow 3/2^- \rightarrow 7/2^- \rightarrow 11/2^-$ or $1/2^+ \rightarrow 3/2^- \rightarrow 5/2^- \rightarrow 9/2^- \rightarrow 11/2^-$ which enhance the isomer population by many orders of magnitude.

Table 4
Gamma decay of the levels in ^{131}Te from the (n,γ) reaction. Gamma energies E_γ are recoil corrected

E_i (keV)	Spin	E_γ (keV)	I_γ (%)	E_f (keV)	Spin
0.00(0)	$3/2^+$				
182.34(4)	$11/2^-$				
296.02(1)	$1/2^+$				
		296.0	47.66	0.0	$3/2^+$
642.32(1)	$5/2^+$				
		642.3	6.36	0.0	$3/2^+$
802.28(4)	$(9/2^-)$				
		619.9	1.11	182.3	$11/2^-$
854.40(2)	$3/2^+$				
		854.4	3.54	0.0	$3/2^+$
		558.2	0.37	296.0	$1/2^+$
		211.8	0.23	642.3	$5/2^+$
880.39(4)	$7/2^-$				
		698.1	3.82	182.3	$11/2^-$
943.45(5)	$7/2^+$				
		943.4	0.55	0.0	$3/2^+$
1041.73(8)	$1/2^+$				
		1041.7	2.77	0.0	$3/2^+$
1050.84(2)	$3/2^+$				
		1050.9	1.97	0.0	$3/2^+$
		754.9	1.36	296.0	$1/2^+$
		408.5	1.49	642.3	$5/2^+$
1207.11(3)	$5/2^+$				
		1207.1	1.76	0.0	$3/2^+$
		910.6	0.32	296.0	$1/2^+$
		352.5	0.03	854.4	$3/2^+$
1267.44(20)	$7/2^+$				
		1267.6	0.13	0.0	$3/2^+$
		625.2	0.19	642.3	$5/2^+$
		324.4	0.06	943.4	$7/2^+$
1398.91(7)	$5/2^+$				
		1399.1	0.74	0.0	$3/2^+$
		756.7	0.72	642.3	$5/2^+$
		544.3	0.03	854.4	$3/2^+$
		455.6	0.09	943.4	$7/2^+$
1469.66(9)	$5/2^+$				
		1469.8	0.78	0.0	$3/2^+$
		525.9	0.10	943.4	$7/2^+$
1659.49(7)	$7/2^-$				
		1477.0	0.22	182.3	$11/2^-$
		857.2	0.56	802.3	$(9/2^-)$
		779.3	0.13	880.4	$7/2^-$
1670.26(21)	(5/2)				
		815.1	0.03	854.4	$3/2^+$
		789.0	0.04	880.4	$7/2^-$
		726.8	0.25	943.4	$7/2^+$
		619.9	0.10	1050.8	$3/2^+$
1678.30(8)	(1/2, 3/2)				
		1678.6	0.13	0.0	$3/2^+$

(*continued on next page*)

Table 4 (*Continued*)

E_i (keV)	Spin	E_γ (keV)	I_γ (%)	E_f (keV)	Spin
		1382.2	0.38	296.0	$1/2^+$
		823.9	0.11	854.4	$3/2^+$
		636.8	0.11	1041.7	$1/2^+$
1683.10(8)	$(1/2, 3/2)$				
		1683.5	1.23	0.0	$3/2^+$
		1040.8	0.92	642.3	$5/2^+$
		828.6	0.52	854.4	$3/2^+$
		632.0	0.17	1050.8	$3/2^+$
1721.63(7)	$(5/2^+)$				
		1721.5	0.76	0.0	$3/2^+$
		1079.6	0.11	642.3	$5/2^+$
		515.0	0.18	1207.1	$5/2^+$
1756.01(5)	$5/2^-$				
		1756.1	0.12	0.0	$3/2^+$
		953.7	0.16	802.3	$(9/2^-)$
		875.6	0.46	880.4	$7/2^-$
1781.22(6)	$3/2^-$				
		1780.9	0.43	0.0	$3/2^+$
		1485.0	0.51	296.0	$1/2^+$
		926.2	0.05	854.4	$3/2^+$
		900.9	0.36	880.4	$7/2^-$
		739.4	0.05	1041.7	$1/2^+$
1787.97(6)	$7/2^-$				
		985.7	0.08	802.3	$(9/2^-)$
		907.6	0.26	880.4	$7/2^-$
1852.51(61)	$(7/2, 9/2)$				
		1050.2	0.02	802.3	$(9/2^-)$
1855.79(7)	$(3/2)$				
		1855.8	0.42	0.0	$3/2^+$
		1213.2	0.06	642.3	$5/2^+$
		1001.0	0.06	854.4	$3/2^+$
		813.4	0.04	1041.7	$1/2^+$
		805.0	0.22	1050.8	$3/2^+$
		457.2	0.05	1398.9	$5/2^+$
1867.07(14)	$7/2^-$				
		1064.7	0.06	802.3	$(9/2^-)$
		986.7	0.13	880.4	$7/2^-$
1951.61(8)	$1/2^+, 3/2$				
		1951.4	0.46	0.0	$3/2^+$
		1309.2	0.10	642.3	$5/2^+$
		1097.4	0.23	854.4	$3/2^+$
		910.0	0.06	1041.7	$1/2^+$
		900.9	0.13	1050.8	$3/2^+$
		744.5	0.21	1207.1	$5/2^+$
		230.0	0.07	1721.6	$(5/2^+)$
2015.46(4)	$5/2^+$				
		2015.9	0.51	0.0	$3/2^+$
		1161.8	0.13	854.4	$3/2^+$
		1135.1	0.28	880.4	$7/2^-$
		807.8	0.12	1207.1	$5/2^+$

(*continued on next page*)

Table 4 (*Continued*)

E_i (keV)	Spin	E_γ (keV)	I_γ (%)	E_f (keV)	Spin
		616.4	0.04	1398.9	$5/2^+$
		545.8	0.04	1469.7	$5/2^+$
		355.9	0.29	1659.5	$7/2^-$
		332.3	0.06	1683.1	$(1/2, 3/2)$
		227.2	0.02	1788.0	$7/2^-$
2092.02(4)	$3/2^-$				
		2092.1	0.63	0.0	$3/2^+$
		1796.0	0.69	296.0	$1/2^+$
		1211.9	0.23	880.4	$7/2^-$
		1041.6	0.06	1050.8	$3/2^+$
		336.0	0.05	1756.0	$5/2^-$
		311.0	0.06	1781.2	$3/2^-$
2231.08(6)	$(1/2^+, 3/2)$				
		2231.1	0.46	0.0	$3/2^+$
		1935.7	0.03	296.0	$1/2^+$
		1588.5	0.21	642.3	$5/2^+$
		1187.3	0.07	1041.7	$1/2^+$
		1180.6	0.10	1050.8	$3/2^+$
		1024.1	0.06	1207.1	$5/2^+$
2330.21(20)	$7/2^-$				
		1528.0	0.23	802.3	$(9/2^-)$
		1450.8	0.23	880.4	$7/2^-$
		670.3	0.12	1659.5	$7/2^-$
2373.86(40)	$7/2^-$				
		1571.7	0.09	802.3	$(9/2^-)$
		1492.9	0.03	880.4	$7/2^-$
2457.17(9)	$3/2^+$				
		2456.8	0.59	0.0	$3/2^+$
		2161.3	0.19	296.0	$1/2^+$
		1603.0	0.29	854.4	$3/2^+$
		1414.3	0.10	1041.7	$1/2^+$
		1405.4	0.18	1050.8	$3/2^+$
		1250.9	0.05	1207.1	$5/2^+$
2496.60(9)	$5/2^+$				
		2200.6	0.23	296.0	$1/2^+$
		1642.4	0.20	854.4	$3/2^+$
		1616.0	0.07	880.4	$7/2^-$
		1230.1	0.09	1267.4	$7/2^+$
		837.1	0.16	1659.5	$7/2^-$
		708.6	0.08	1788.0	$7/2^-$
2512.00(3)	$3/2^-$				
		2512.1	3.25	0.0	$3/2^+$
		2215.9	4.51	296.0	$1/2^+$
		1470.3	0.11	1041.7	$1/2^+$
		1459.7	0.03	1050.8	$3/2^+$
		1304.0	0.06	1207.1	$5/2^+$
		853.3	0.05	1659.5	$7/2^-$
		829.2	0.09	1683.1	$(1/2, 3/2)$
		755.5	0.05	1756.0	$5/2^-$
		496.6	0.04	2015.5	$5/2^+$

(*continued on next page*)

Table 4 (*Continued*)

E_i (keV)	Spin	E_γ (keV)	I_γ (%)	E_f (keV)	Spin
		419.9	0.04	2092.0	$3/2^-$
2544.26(12)	$(7/2^+)$				
		1901.2	0.08	642.3	$5/2^+$
		1742.1	0.15	802.3	$(9/2^-)$
		1689.4	0.25	854.4	$3/2^+$
		1663.9	0.19	880.4	$7/2^-$
		1277.4	0.12	1267.4	$7/2^+$
2547.71(9)	$3/2^-$				
		2548.3	0.48	0.0	$3/2^+$
		2251.5	0.14	296.0	$1/2^+$
		1905.0	0.18	642.3	$5/2^+$
		1505.3	0.06	1041.7	$1/2^+$
		1496.8	0.14	1050.8	$3/2^+$
		791.6	0.19	1756.0	$5/2^-$
2582.54(2)	$3/2^-$				
		2582.6	4.87	0.0	$3/2^+$
		2286.5	26.77	296.0	$1/2^+$
		1940.5	0.37	642.3	$5/2^+$
		1702.5	0.40	880.4	$7/2^-$
		1540.6	0.14	1041.7	$1/2^+$
		1531.7	0.60	1050.8	$3/2^+$
		1375.1	0.04	1207.1	$5/2^+$
		1183.7	0.30	1398.9	$5/2^+$
		1112.8	0.23	1469.7	$5/2^+$
		860.7	0.08	1721.6	$(5/2^+)$
		567.1	0.33	2015.5	$5/2^+$
		490.7	0.17	2092.0	$3/2^-$
2671.36(18)	1/2, 3/2				
		2671.4	0.18	0.0	$3/2^+$
		1817.4	0.12	854.4	$3/2^+$
		1629.7	0.06	1041.7	$1/2^+$
2706.32(7)	$3/2^-$				
		2706.4	0.10	0.0	$3/2^+$
		2410.1	0.45	296.0	$1/2^+$
		1665.0	0.09	1041.7	$1/2^+$
		950.6	0.06	1756.0	$5/2^-$
2754.25(7)	$3/2^-$				
		2754.1	0.09	0.0	$3/2^+$
		1873.8	0.34	880.4	$7/2^-$
		1703.3	0.09	1050.8	$3/2^+$
		1076.0	0.28	1678.3	(1/2, 3/2)
		1071.8	0.12	1683.1	(1/2, 3/2)
		998.3	0.05	1756.0	$5/2^-$
		738.9	0.31	2015.5	$5/2^+$
		661.9	0.13	2092.0	$3/2^-$
2932.48(9)	$1/2^-$				
		2932.9	0.17	0.0	$3/2^+$
		2636.2	0.12	296.0	$1/2^+$
		1890.6	0.15	1041.7	$1/2^+$
		1151.1	0.30	1781.2	$3/2^-$

(*continued on next page*)

Table 4 (*Continued*)

E_i (keV)	Spin	E_γ (keV)	I_γ (%)	E_f (keV)	Spin
		475.3	0.14	2457.2	$3/2^+$
3001.96(3)	$1/2^-$				
		3001.9	4.84	0.0	$3/2^+$
		2705.9	7.18	296.0	$1/2^+$
		2147.5	0.26	854.4	$3/2^+$
		1960.2	0.14	1041.7	$1/2^+$
		1951.1	1.49	1050.8	$3/2^+$
		490.0	0.15	2512.0	$3/2^-$
		419.4	0.46	2582.5	$3/2^-$
3146.23(19)	1/2, 3/2				
		3146.1	0.05	0.0	$3/2^+$
		2291.9	0.06	854.4	$3/2^+$
3170.76(24)	(3/2)				
		3170.6	0.11	0.0	$3/2^+$
3186.71(17)	(3/2)				
		2544.3	0.07	642.3	$5/2^+$
		2332.1	0.07	854.4	$3/2^+$
		2144.1	0.20	1041.7	$1/2^+$
		1405.7	0.07	1781.2	$3/2^-$
		1170.9	0.07	2015.5	$5/2^+$
3507.48(9)	(3/2)				
		3507.7	0.14	0.0	$3/2^+$
		2652.8	0.09	854.4	$3/2^+$
		1751.5	0.28	1756.0	$5/2^-$
3546.87(11)	$3/2^-$				
		3547.2	0.41	0.0	$3/2^+$
		3250.9	0.06	296.0	$1/2^+$
		2903.0	0.03	642.3	$5/2^+$
		2691.2	0.04	854.4	$3/2^+$
		2665.1	0.18	880.4	$7/2^-$
		2504.7	0.14	1041.7	$1/2^+$
		2495.5	0.22	1050.8	$3/2^+$
3568.27(5)	$3/2^-$				
		3568.2	0.25	0.0	$3/2^+$
		3271.7	0.06	296.0	$1/2^+$
		2925.7	0.66	642.3	$5/2^+$
		2713.7	0.09	854.4	$3/2^+$
		2689.3	0.07	880.4	$7/2^-$
		2361.1	0.25	1207.1	$5/2^+$
		2097.2	0.10	1469.7	$5/2^+$
		1476.3	0.05	2092.0	$3/2^-$
		1071.8	0.09	2496.6	$5/2^+$
		861.6	0.09	2706.3	$3/2^-$
3601.66(11)	$3/2^-$				
		3602.1	0.28	0.0	$3/2^+$
		3305.5	0.33	296.0	$1/2^+$
		2959.3	0.24	642.3	$5/2^+$
		2746.2	0.09	854.4	$3/2^+$
		2549.7	0.18	1050.8	$3/2^+$
		1019.5	0.14	2582.5	$3/2^-$

(*continued on next page*)

Table 4 (*Continued*)

E_i (keV)	Spin	E_γ (keV)	I_γ (%)	E_f (keV)	Spin
3623.72(7)	$3/2^-$				
		3623.4	0.08	0.0	$3/2^+$
		3327.5	0.67	296.0	$1/2^+$
		2768.3	0.04	854.4	$3/2^+$
		2743.4	0.11	880.4	$7/2^-$
		2581.9	0.13	1041.7	$1/2^+$
		1608.3	0.20	2015.5	$5/2^+$
		1532.3	0.06	2092.0	$3/2^-$
		1292.7	0.18	2330.2	$7/2^-$
		917.5	0.19	2706.3	$3/2^-$
		868.1	0.14	2754.2	$3/2^-$
3668.25(10)	$3/2^-$				
		3667.9	0.47	0.0	$3/2^+$
		3372.5	0.09	296.0	$1/2^+$
		3026.0	0.09	642.3	$5/2^+$
		2617.7	0.09	1050.8	$3/2^+$
		2269.8	0.05	1398.9	$5/2^+$
3689.79(7)	$1/2^-$				
		3690.0	1.38	0.0	$3/2^+$
		3394.0	0.17	296.0	$1/2^+$
		2648.4	0.07	1041.7	$1/2^+$
		1737.9	0.08	1951.6	$1/2^+, 3/2$
		1359.3	0.25	2330.2	$7/2^-$
3698.27(6)	$3/2^-$				
		3698.2	0.46	0.0	$3/2^+$
		3402.4	0.17	296.0	$1/2^+$
		3055.2	0.05	642.3	$5/2^+$
		2647.1	0.10	1050.8	$3/2^+$
		1241.1	0.08	2457.2	$3/2^+$
3737.84(11)	(3/2)				
		3442.1	0.01	296.0	$1/2^+$
		3095.7	0.05	642.3	$5/2^+$
		2685.9	0.01	1050.8	$3/2^+$
		2530.6	0.06	1207.1	$5/2^+$
		1226.2	0.11	2512.0	$3/2^-$
3763.42(15)	$3/2^-$				
		3762.9	0.09	0.0	$3/2^+$
		3468.6	0.09	296.0	$1/2^+$
3938.59(7)	$3/2^-$				
		3938.9	0.37	0.0	$3/2^+$
		3642.5	0.88	296.0	$1/2^+$
		3058.8	0.06	880.4	$7/2^-$
3987.01(22)	$3/2^-$				
		3987.0	0.15	0.0	$3/2^+$
		3691.2	0.18	296.0	$1/2^+$
		3132.0	0.09	854.4	$3/2^+$
4028.37(13)	(3/2)				
		4028.7	0.09	0.0	$3/2^+$
		3732.5	0.09	296.0	$1/2^+$
		3175.1	0.08	854.4	$3/2^+$

(*continued on next page*)

Table 4 (*Continued*)

E_i (keV)	Spin	E_γ (keV)	I_γ (%)	E_f (keV)	Spin
		1515.6	0.12	2512.0	$3/2^-$
4036.63(5)	$3/2^-$				
		4036.4	0.11	0.0	$3/2^+$
		3740.5	0.72	296.0	$1/2^+$
		3394.0	0.07	642.3	$5/2^+$
		3181.1	0.10	854.4	$3/2^+$
		3155.4	0.23	880.4	$7/2^-$
		2828.8	0.06	1207.1	$5/2^+$
4061.18(18)	$1/2^-$				
		4060.8	0.13	0.0	$3/2^+$
4070.40(6)	$3/2^-$				
		4070.6	0.11	0.0	$3/2^+$
		3774.5	0.79	296.0	$1/2^+$
		3189.9	0.12	880.4	$7/2^-$
		3030.2	0.02	1041.7	$1/2^+$
		3019.9	0.04	1050.8	$3/2^+$
		2863.2	0.13	1207.1	$5/2^+$
		2599.8	0.06	1469.7	$5/2^+$
		2349.2	0.15	1721.6	$(5/2^+)$
4109.00(8)	$3/2^-$				
		4109.2	0.44	0.0	$3/2^+$
		3812.3	0.09	296.0	$1/2^+$
4124.33(19)	$3/2^-$				
		3482.6	0.06	642.3	$5/2^+$
4238.98(15)	$1/2^-$				
		4240.0	0.33	0.0	$3/2^+$
		3944.1	0.28	296.0	$1/2^+$
		2556.4	0.09	1683.1	$(1/2, 3/2)$
		1484.0	0.09	2754.2	$3/2^-$
4253.59(6)	$1/2^-$				
		4253.7	0.34	0.0	$3/2^+$
		3957.7	0.42	296.0	$1/2^+$
		3212.6	0.09	1041.7	$1/2^+$
		3203.6	0.06	1050.8	$3/2^+$
		2472.6	0.08	1781.2	$3/2^-$
		2162.3	0.11	2092.0	$3/2^-$
4278.62(15)	$3/2^-$				
		4279.0	0.19	0.0	$3/2^+$
		3981.8	0.12	296.0	$1/2^+$
		3635.7	0.18	642.3	$5/2^+$
		1524.6	0.11	2754.2	$3/2^-$
4285.80(6)	$3/2^-$				
		4287.2	0.04	0.0	$3/2^+$
		3989.7	0.84	296.0	$1/2^+$
		3643.7	0.06	642.3	$5/2^+$
		3405.7	0.06	880.4	$7/2^-$
		3234.2	0.06	1050.8	$3/2^+$
		1737.9	0.08	2547.7	$3/2^-$
4300.28(6)	$3/2^-$				
		4004.4	0.18	296.0	$1/2^+$

(*continued on next page*)

Table 4 (*Continued*)

E_i (keV)	Spin	E_γ (keV)	I_γ (%)	E_f (keV)	Spin
		3658.6	0.05	642.3	$5/2^+$
		3257.9	0.06	1041.7	$1/2^+$
		3250.0	0.04	1050.8	$3/2^+$
		2830.6	0.06	1469.7	$5/2^+$
4324.59(7)	$3/2^-$				
		4028.9	0.23	296.0	$1/2^+$
		3682.5	0.11	642.3	$5/2^+$
		3471.8	0.06	854.4	$3/2^+$
		3283.1	0.11	1041.7	$1/2^+$
		3273.5	0.05	1050.8	$3/2^+$
4364.65(8)	$3/2^-$				
		4364.3	0.02	0.0	$3/2^+$
		4069.1	0.05	296.0	$1/2^+$
		3483.5	0.02	880.4	$7/2^-$
4425.07(12)	(3/2)				
		3571.5	0.07	854.4	$3/2^+$
4436.83(34)	$3/2^-$				
		4438.1	0.09	0.0	$3/2^+$
4445.79(24)	$3/2^-$				
		4445.9	0.15	0.0	$3/2^+$
		4149.5	0.25	296.0	$1/2^+$
4453.80(36)	$1/2^-$				
		4454.2	0.11	0.0	$3/2^+$
		4157.8	0.08	296.0	$1/2^+$
4472.57(10)	$3/2^-$				
		4176.4	0.16	296.0	$1/2^+$
		3831.1	0.02	642.3	$5/2^+$
		3592.4	0.06	880.4	$7/2^-$
4485.25(14)	$3/2^-$				
		4188.3	0.09	296.0	$1/2^+$
		2705.1	0.09	1781.2	$3/2^-$
		1483.0	0.09	3002.0	$1/2^-$
4489.51(20)	(1/2, 3/2)				
		4489.3	0.06	0.0	$3/2^+$
		4193.6	0.26	296.0	$1/2^+$
		3447.9	0.10	1041.7	$1/2^+$
		3437.7	0.06	1050.8	$3/2^+$
		1488.4	0.06	3002.0	$1/2^-$
4519.98(9)	(3/2)				
		4520.0	0.13	0.0	$3/2^+$
		4224.6	0.18	296.0	$1/2^+$
		3478.7	0.15	1041.7	$1/2^+$
		3471.4	0.11	1050.8	$3/2^+$
		3312.8	0.04	1207.1	$5/2^+$
4531.44(10)	$1/2^-$				
		4531.6	0.42	0.0	$3/2^+$
4545.18(7)	$1/2^-$				
		4545.5	1.54	0.0	$3/2^+$
		4249.6	0.69	296.0	$1/2^+$
		3691.0	0.18	854.4	$3/2^+$

(*continued on next page*)

Table 4 (*Continued*)

E_i (keV)	Spin	E_γ (keV)	I_γ (%)	E_f (keV)	Spin
		1542.8	0.20	3002.0	$1/2^-$
4558.45(6)	$1/2^-$				
		4558.7	0.82	0.0	$3/2^+$
		1556.5	0.18	3002.0	$1/2^-$
4563.18(6)	$3/2^-$				
		4563.2	0.17	0.0	$3/2^+$
		4267.1	0.41	296.0	$1/2^+$
		3921.6	0.06	642.3	$5/2^+$
		3683.5	0.07	880.4	$7/2^-$
		3512.0	0.04	1050.8	$3/2^+$
4583.14(12)	$3/2^-$				
		4582.2	0.02	0.0	$3/2^+$
		4287.1	0.09	296.0	$1/2^+$
		3533.4	0.04	1050.8	$3/2^+$
4645.36(6)	$3/2^-$				
		4646.1	0.35	0.0	$3/2^+$
		4349.6	0.21	296.0	$1/2^+$
		3791.6	0.02	854.4	$3/2^+$
		3175.5	0.05	1469.7	$5/2^+$
4649.93(9)	$3/2^-$				
		4650.0	0.04	0.0	$3/2^+$
		4354.1	0.03	296.0	$1/2^+$
4707.46(19)	$(3/2, 5/2)^+$				
		4065.2	0.05	642.3	$5/2^+$
		3499.8	0.03	1207.1	$5/2^+$
		2927.0	0.05	1781.2	$3/2^-$
		1159.2	0.14	3546.9	$3/2^-$
4732.74(18)	$3/2^-$				
		4733.2	0.14	0.0	$3/2^+$
		4092.3	0.07	642.3	$5/2^+$
		3527.0	0.14	1207.1	$5/2^+$
4801.23(12)	$(3/2)$				
		3759.5	0.06	1041.7	$1/2^+$
4856.13(29)	$(3/2^+)$				
		4559.0	0.06	296.0	$1/2^+$
		4214.4	0.05	642.3	$5/2^+$
4869.68(10)	$(3/2)$				
		4870.2	0.35	0.0	$3/2^+$
		4574.7	0.07	296.0	$1/2^+$
4894.05(16)	$(3/2)$				
		4597.3	0.20	296.0	$1/2^+$
4944.92(10)	$3/2^-$				
		4649.0	0.08	296.0	$1/2^+$
		3737.8	0.05	1207.1	$5/2^+$
4964.21(14)	$3/2^-$				
		4668.2	0.09	296.0	$1/2^+$
4970.36(11)	$3/2^-$				
		4674.5	0.12	296.0	$1/2^+$
		4325.0	0.05	642.3	$5/2^+$
5048.55(15)	$(3/2)$				

(*continued on next page*)

Table 4 (*Continued*)

E_i (keV)	Spin	E_γ (keV)	I_γ (%)	E_f (keV)	Spin
		5048.1	0.14	0.0	$3/2^+$
5172.23(25)	(3/2)				
		5172.5	0.14	0.0	$3/2^+$
		4876.7	0.10	296.0	$1/2^+$
5929.38(2)	$1/2^+$				
		5075.0	0.66	854.4	$3/2^+$
		4887.9	0.30	1041.7	$1/2^+$
		4877.4	0.14	1050.8	$3/2^+$
		4721.9	0.12	1207.1	$5/2^+$
		4246.6	1.26	1683.1	$(1/2, 3/2)$
		4207.4	0.39	1721.6	$(5/2^+)$
		4148.2	0.04	1781.2	$3/2^-$
		4073.5	0.38	1855.8	(3/2)
		3978.3	0.36	1951.6	$1/2^+, 3/2$
		3912.7	0.54	2015.5	$5/2^+$
		3837.3	0.37	2092.0	$3/2^-$
		3698.2	0.46	2231.1	$(1/2^+, 3/2)$
		3471.0	0.37	2457.2	$3/2^+$
		3417.4	7.82	2512.0	$3/2^-$
		3381.6	0.75	2547.7	$3/2^-$
		3346.8	32.03	2582.5	$3/2^-$
		3258.3	0.15	2671.4	$1/2, 3/2$
		3223.0	1.01	2706.3	$3/2^-$
		3175.3	1.17	2754.2	$3/2^-$
		2996.6	0.90	2932.5	$1/2^-$
		2927.4	14.71	3002.0	$1/2^-$
		2783.1	0.23	3146.2	$1/2, 3/2$
		2758.6	0.21	3170.8	(3/2)
		2742.4	0.32	3186.7	(3/2)
		2422.0	0.34	3507.5	(3/2)
		2382.5	1.04	3546.9	$3/2^-$
		2361.1	1.77	3568.3	$3/2^-$
		2327.6	1.41	3601.7	$3/2^-$
		2305.6	1.14	3623.7	$3/2^-$
		2261.1	0.55	3668.2	$3/2^-$
		2239.7	1.98	3689.8	$1/2^-$
		2231.1	0.46	3698.3	$3/2^-$
		2191.6	0.35	3737.8	(3/2)
		2166.0	0.38	3763.4	$3/2^-$
		1990.8	0.80	3938.6	$3/2^-$
		1942.5	0.46	3987.0	$3/2^-$
		1901.0	0.39	4028.4	(3/2)
		1892.7	1.50	4036.6	$3/2^-$
		1868.1	0.26	4061.2	$1/2^-$
		1859.0	1.73	4070.4	$3/2^-$
		1820.4	0.57	4109.0	$3/2^-$
		1805.1	0.29	4124.3	$3/2^-$
		1690.5	1.10	4239.0	$1/2^-$
		1675.8	0.90	4253.6	$1/2^-$
		1650.7	0.36	4278.6	$3/2^-$

(*continued on next page*)

Table 4 (*Continued*)

E_i (keV)	Spin	E_γ (keV)	I_γ (%)	E_f (keV)	Spin
		1643.6	1.37	4285.8	$3/2^-$
		1629.1	0.58	4300.3	$3/2^-$
		1604.8	0.55	4324.6	$3/2^-$
		1564.7	0.40	4364.6	$3/2^-$
		1504.3	0.27	4425.1	$(3/2)$
		1492.6	0.09	4436.8	$3/2^-$
		1483.5	0.37	4445.8	$3/2^-$
		1475.7	0.11	4453.8	$1/2^-$
		1456.8	0.42	4472.6	$3/2^-$
		1444.1	0.24	4485.3	$3/2^-$
		1440.4	0.55	4489.5	$(1/2, 3/2)$
		1409.4	0.43	4520.0	$(3/2)$
		1398.0	0.32	4531.4	$1/2^-$
		1384.2	2.80	4545.2	$1/2^-$
		1371.0	1.34	4558.4	$1/2^-$
		1366.2	0.91	4563.2	$3/2^-$
		1346.2	0.22	4583.1	$3/2^-$
		1284.0	0.73	4645.4	$3/2^-$
		1279.5	0.30	4649.9	$3/2^-$
		1221.9	0.19	4707.5	$(3/2, 5/2)^+$
		1196.7	0.42	4732.7	$3/2^-$
		1128.1	0.18	4801.2	$(3/2)$
		1073.2	0.18	4856.1	$(3/2^+)$
		1059.7	0.21	4869.7	$(3/2)$
		1035.3	0.20	4894.0	$(3/2)$
		984.5	0.33	4944.9	$3/2^-$
		965.2	0.17	4964.2	$3/2^-$
		959.0	0.35	4970.4	$3/2^-$
		880.8	0.14	5048.6	$(3/2)$
		757.3	0.14	5172.2	$(3/2)$

The energies of the levels given in Table 1 were determined with a least squares fit to the transition energies with program LEVFIT [29]. The neutron binding energy was determined with this program to be 5929.376(23) keV with an additional systematic error of 0.05 keV. This value is in good agreement with the evaluated neutron separation energy, 5929.7(5) keV [30].

4. Level scheme

The construction of the level scheme of ^{131}Te is based mainly on the present experimental data from the (d, p) reaction and the (n, γ) coincidence measurement in combination with previous data given in the nuclear data sheets [11].

Spin and parity assignments for most of the levels result from the angular distributions and asymmetries of the (d, p) reaction. Additional restrictions of spin and parity follow from the (n, γ) transitions assuming that primary transitions have E1, M1 or

only exceptionally E2 multipolarity and secondary transitions can have E1, M1 or E2 characteristic.

All levels observed in previous transfer reaction experiments were confirmed by our new (d, p) results. In many cases we establish for the first time the γ decay of these levels. However, many levels which were only constructed with γ lines from β decay could not be substantiated by our new data (1037, 1467, 1545, 1601, 1854, 1876, 2067, 2180, 2226, 2335, 2398, 2496, 2552, 2599 and 2662 keV). The corresponding γ lines were either placed somewhere else or not observed. The reason might be that the decay of the $7/2^+$ ground state of ^{131}Sb goes mainly to higher spin states in ^{131}Te which are only weakly populated in the (n, γ) reaction, or these β decay levels do not exist. The previous (n, γ) measurements are essentially in agreement with the new more sensitive experiments.

Comments to some levels:

The 776.88 keV level This level was introduced in the level scheme in Ref. [20] with respect to four feeding transitions and coincidence relations between the 642 keV, 134 keV and 274 keV transitions. However, we observed no evidence for this level neither in the (d, p) spectra nor in the γ-single and -coincidence spectra. Thus, we assume that the lack of the evidence in the present study is either due to a complicated structure of this level and its high spin, $\geqslant 9/2$, or due to nonexistence of this level.

The 802.28 keV level We obtained evidence for this new level in the proton spectra as well as in the (n, γ) measurement. While a very weak population of this level in the (d, p) reaction does not enable us to determine definite spin and parity to this level the feeding and decay pattern of this level observed in the γ decay following thermal neutron capture point to a $9/2^-$ member of the $h_{11/2}$ family of states. This assignment is also supported by the systematics of the odd-Te isotopes [2].

The 854.44 keV level While Shahabuddin et al. [18] suggested the transfer momentum in the (t, d) reaction $l = 0$ for this level our (d, p) data exclude this assignment. There is not a minimum at 17° in the angular distribution of the partial cross section and all experimental points in the angular distribution of the asymmetry are positive (see Fig. 2). On the other hand, our data are fitted rather well with DWBA curves for $l = 2$ and $3/2^+$ (see Fig. 3).

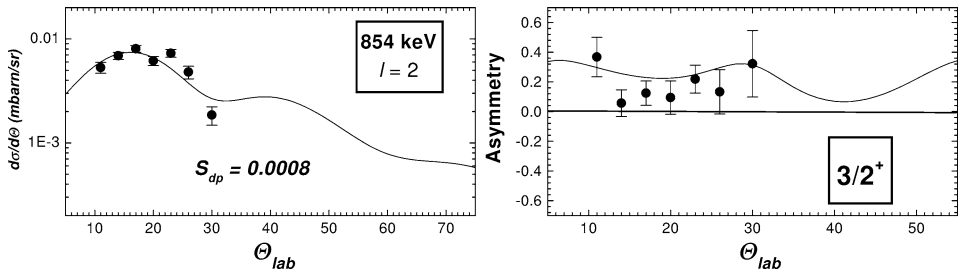

Fig. 3. Angular distributions for the level at 854 keV and DWBA fit. Note: the lines associated with this level in the proton spectra at scattering angles higher than 30° suffer interference with lines from tungsten.

The 1398.92 level Level energies following from our (d, p) and (n, γ) data agree with the value given from the β-decay measurements [19,20]. Our spin and parity assignment is also not in contradiction with suggestion from β-decay experiments. The levels seen in the previous neutron stripping reaction studies [16,18] at 1400 keV could be the same level which was observed in our stripping reaction and β-decay, despite the different transfer momentum l given in our work and Ref. [18]. Thus, the presence of an additional level at 1400 keV in the level scheme is at least questionable.

The 1659 keV level The $7/2^-$ assignment following from the present (d, p) experiment is supported by γ transitions going from this level to the $11/2^-$ and $(9/2^-)$ levels at 182 and 802 keV, respectively.

The 1841.9 keV level The negative asymmetry for this level clearly points to a $5/2^+$ or $7/2^-$ assignment. As our (d, p) data slightly prefer a transfer momentum $l = 2$ to $l = 3$ which was suggested in Ref. [18] for this level we adopted both possible assignments, $5/2^+$ or $7/2^-$.

The 1867.04 keV level Similar angular distributions for $l = 2$ and $l = 3$ and interference with tungsten lines at some scattering angles do not allow to arrive at a unique value of l. However, analyzing our (d, p) data we can exclude $l = 0$ for this level suggested in Ref. [18]. The angular distributions of the asymmetries reduce possible spin and parity values to $7/2^-$ and $5/2^+$. On the other hand, we observed the γ transition to the 802 keV level with spin and parity $(9/2^-)$. Thus, the $5/2^+$ assignment seems to be less probable and even should be disregarded.

The 2015.45 keV level In spite of a different transfer momentum observed in the present work the level observed in our proton and γ spectra at 2016.1 keV and at 2015.45 keV is probably identical with states at 2014 keV by Graue et al. [16] and Shahabuddin et al. [18]. While in both previous neutron stripping reactions the value of the transfer momentum $l = 1$ was reported, we arrive at spin-parity $5/2^+$ for this level. This $5/2^+$ assignment is not in contradiction with the deduced feedings of 2017.0 ± 0.6 keV level suggested in the work by Hnatowicz et al. [20] and omitted in NDS [11] due to inconsistency with $l = 1$. The 3912.7 ± 0.5 keV primary transition seems to be an E2 transition.

5. Comparison with theoretical models

The rich experimental results obtained for this nucleus will be compared with calculations performed with two theoretical models: the Interacting Boson–Fermion Model (IBFM) [31] and the Quasiparticle Phonon Model (QPM) [32]. Although we expect that only the lowest excited states will be reasonably well described by the former model, and that the later model will give an overall better description, in particular for the higher excited states, a comparison of their results is worthwhile in order to assess the structure of the observed states.

5.1. The interacting boson–fermion model calculations

The systematics of the lowest excited states of both parities shows that ^{131}Te continues rather smoothly the evolution observed along the isotopic chain from ^{119}Te to ^{129}Te briefly presented in [2]. Since for the lighter isotopes a reasonable description of the observed trend was obtained with the IBFM, we extend first such a description to ^{131}Te.

Nevertheless, the ^{131}Te nucleus is somewhat at the limit of applicability of the IBFM, due to its vicinity to the closed shell. We describe this nucleus as consisting of a ^{132}Te core to which one couples an odd nucleon hole which may occupy any of the valence space shell model orbitals. In the IBM description, ^{132}Te ($Z = 52$, $N = 80$) has only two bosons: one proton boson and one neutron boson; in such a small boson space one can build, besides the 0^+ ground state, only another 0^+ state, two 2^+ states, and one 4^+ state. This rather restricted number of core states, when coupled with the odd fermion, will be expected to produce a too small number of states in the odd nucleus at higher excitation energies (the 'boson cut-off' effect).

For the description of the ^{132}Te core we have chosen IBM parameter values smoothly extrapolated from the other lighter isotopes [2]: $\varepsilon' = 0.96$, $c'(0, 2, 4) = (0.2, 0.0, 0.0)$, $v_2 = 0.071$ and $v_0 = -0.08$ (all in MeV). This extrapolation was necessary since in ^{132}Te no excited states with spin unambiguously lower than 4 are known except for the 2^+ state, and the known 4_1^+ state is very likely not the expected collective one [33].

The odd neutron was allowed to occupy the spherical shell model orbitals of the 50–82 shell ($2d_{5/2}$, $1g_{7/2}$, $3s_{1/2}$, $2d_{3/2}$ and $1h_{11/2}$) and some orbitals of the next major shell: $2f_{7/2}$, $3p_{3/2}$, $1h_{9/2}$, $3p_{1/2}$. The single particle energies were also chosen from a smooth extrapolation of those of the lighter isotopes [2]. For the calculation of one-neutron transfer spectroscopic factors we used the program SPEC [34] with the transfer operator described in Ref. [35].

Since the whole chain from mass 119 to 129 could be described with essentially the same boson–fermion interaction parameters, the first explorative calculation for ^{131}Te was made with the same values: the monopole–monopole, quadrupole–quadrupole, and exchange interaction strength parameters were $A_0 = -0.2$ MeV, $\Gamma_0 = 0.2$ MeV, and $\Lambda_0 = 0.95$ MeV^2, respectively, for both the positive and negative parity states. This calculation gave a reasonable description of the low energy (below ~ 1.7 MeV) level positions, as well as their gamma-ray decay. The spectroscopic factors of the most strongly populated states $3/2_1^+$, $11/2_1^-$, and $1/2_1^+$ were also very well reproduced. On the other hand, the observed fragmentation of the $d_{5/2}$ and $g_{7/2}$ orbitals among states between 600 and 1600 keV excitation (Fig. 5 discussed below) could not be reproduced. For all these states the predicted spectroscopic factors S_{lj} are very low, close to or below 10^{-5}. The observed larger S_{lj} values for these states are indicative of a larger participation of the $d_{5/2}$ and $g_{7/2}$ orbitals in their wavefunctions. To achieve this within the model, we have increased the boson–fermion interaction, which is especially effective to increase the quadrupole–quadrupole interaction strength. The results presented below are obtained with a value $\Gamma_0 = 0.35$ MeV. Fig. 4 shows the comparison between the experimental and calculated level schemes, all the states up to 2.5 MeV excitation being shown in both cases. Table 5 completes this figure with information concerning the electromagnetic decay properties of some states, while Fig. 5 shows the one neutron stripping spectroscopic

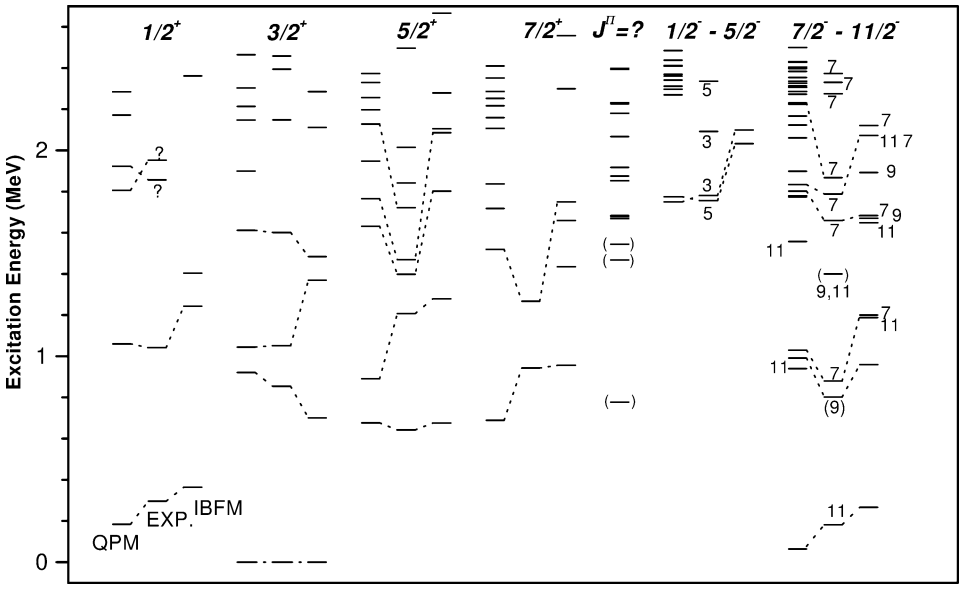

Fig. 4. Comparison between the experimental levels and the IBFM and QPM predictions. Below 2.5 MeV, all known experimental levels and all calculated levels are shown. The correspondences between experimental levels and calculated states are based on the level positions, their electromagnetic decay properties and their neutron-transfer spectroscopic strengths. The levels in brackets are uncertain. The question marks denote uncertain spin-parity assignments.

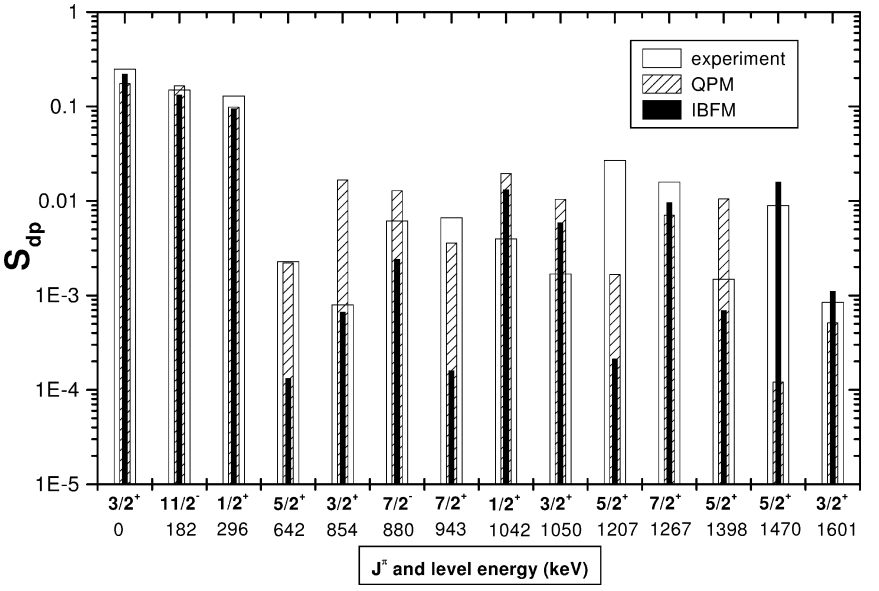

Fig. 5. Comparison between the experimental (d, p) spectroscopic strength and the IBFM and QPM calculation predictions.

Table 5
Experimental and theoretical electromagnetic properties of ^{131}Te states. The IBFM and QPM branchings have been calculated with the experimental level energies. Only branchings with at least one value larger than 0.1% are presented

E_x (MeV)	J_i	J_f	E_γ (MeV)	Exp.	IBFM	QPM
		Positive parity states				
0.296	$1/2_1$	$3/2_1$	0.296	100	100	100
0.642	$5/2_1$	$3/2_1$	0.642	100	100	100
		$1/2_1$	0.346	–	0.4	1.3
0.854	$3/2_2$	$3/2_1$	0.854	100	100	100
		$1/2_1$	0.558	3.9	5.6	–
		$5/2_1$	0.212	15.2	19.3	–
0.943	$7/2_1$	$3/2_1$	0.943	100	100	100
		$5/2_1$	0.301	5.1	4.6	–
1.041	$1/2_2$	$3/2_1$	1.041	100	100	100
		$1/2_1$	0.745	32.9	97.8	–
		$5/2_1$	0.398	–	–	0.1
		$3/2_2$	0.186	–	4.5	–
1.051	$3/2_3$	$3/2_1$	1.051	100	100	10.7
		$1/2_1$	0.754	70.9	77.0	100
		$5/2_1$	0.409	75.6	40.8	0.9
		$3/2_2$	0.196	–	10.8	–
1.207	$5/2_2$	$3/2_1$	1.207	100	100	100
		$1/2_1$	0.911	18.3	12.1	18.2
		$5/2_1$	0.565	–	19.2	–
		$3/2_2$	0.353	1.6	6.7	–
		$7/2_1$	0.263	–	0.1	–
		$3/2_3$	0.156	–	1.1	–
1.268	$7/2_2$	$3/2_1$	1.268	66.7	100	100
		$5/2_1$	0.625	100	67.5	83.0
		$3/2_2$	0.413	–	0.1	0.5
		$7/2_1$	0.263	28.6	17.9	69.3
		$3/2_3$	0.156	–	–	0.3
		$5/2_2$	0.061	–	–	0.1
1.399	$5/2_3$	$3/2_1$	1.399	100	100	–
		$1/2_1$	1.103	–	1.5	7.0
		$5/2_1$	0.757	100	1.9	100
		$3/2_2$	0.545	3.8	0.9	8.1
		$7/2_1$	0.455	12.5	0.1	1.7
		$1/2_2$	0.357	–	–	0.8
		$3/2_3$	0.348	–	1.9	0.1
		$5/2_2$	0.192	–	–	0.1
1.470	$5/2_4$	$3/2_1$	1.470	100	100	100
		$1/2_1$	1.173	–	0.3	34.2
		$5/2_1$	0.827	–	2.4	1.7
		$3/2_2$	0.615	–	0.2	2.1
		$7/2_1$	0.526	12.9	0.1	1.2
		$7/2_2$	0.202	–	0.2	–
1.722	$5/2_5$	$3/2_1$	1.722	100	2.5	100
		$1/2_1$	1.426	–	0.2	7.6
		$5/2_1$	1.079	–	100	22.8
		$3/2_2$	0.867	–	3.2	0.3

(*continued on next page*)

Table 5 (*Continued*)

E_x (MeV)	J_i	J_f	E_γ (MeV)	Exp.	IBFM	QPM
		$7/2_1$	0.778	14.5	12.2	2.1
		$1/2_2$	0.680	–	9.9	0.7
		$3/2_3$	0.671	–	20.7	2.7
		$5/2_2$	0.515	24.2	3.3	1.9
		$7/2_2$	0.454	–	7.3	–
		$5/2_3$	0.323	–	33.2	–
1.856	$1/2_3$	$3/2_1$	1.856	100	–	100
		$5/2_1$	1.214	14.3	–	–
		$3/2_2$	1.002	14.3	–	2.6
		$1/2_2$	0.815	9.5	–	–
		$3/2_3$	0.805	52.4	–	1.8
		$5/2_2$	0.649	–	–	0.9
		$5/2_3$	0.457	11.9	–	0.1
1.952	$1/2_4$	$3/2_1$	1.952	100	–	100
		$5/2_1$	1.310	21.7	–	0.1
		$3/2_2$	1.098	50.0	–	28.0
		$1/2_2$	0.911	13.0	–	–
		$3/2_3$	0.901	28.3	–	25.9
		$5/2_2$	0.745	45.6	–	0.2
		$5/2_5$	0.230	15.2	–	0.4
			Negative parity states			
0.802	$9/2_1$	$11/2_1$	0.620	100	100	100
0.880	$7/2_1$	$11/2_1$	0.698	100	100	100
		$9/2_1$	0.078	–	1.6	–
1.660	$7/2_2$	$11/2_1$	1.477	38.7	0.2	48.4
		$9/2_1$	0.857	100	100	98.5
		$7/2_1$	0.779	8.1	6.3	100
1.756	$5/2_1$	$9/2_1$	0.953	33.3	45.4	16.7
		$7/2_1$	0.876	100	100	100
		$7/2_2$	0.097	–	2.9	–
1.781	$3/2_1$	$7/2_1$	0.901	100	100	100
		$5/2_1$	0.025	–	0.1	–
1.788	$7/2_3$	$11/2_1$	1.606	–	37.6	52.5
		$9/2_1$	0.986	32.1	22.5	100
		$7/2_1$	0.908	100	100	15.6
		$7/2_2$	0.129	–	0.4	–
1.867	$7/2_4$	$11/2_1$	1.685	–	–	13.3
		$9/2_1$	1.065	46	–	92.8
		$7/2_1$	0.987	100	–	100
2.092	$3/2_2$	$7/2_1$	1.212	100	100	100
		$5/2_1$	0.336	20.1	0.9	–
		$7/2_3$	0.304	–	0.1	–

factors. Taking into account all these data, the correspondences shown in Fig. 4 can be made between experimental and calculated levels. One should note that, since we have used the same Hamiltonian for both the positive and negative parity states, we can also compare the absolute excitation energy of the lowest negative parity state $11/2^-$: it is predicted at 267 keV, which compares well with the experimental value of 182 keV.

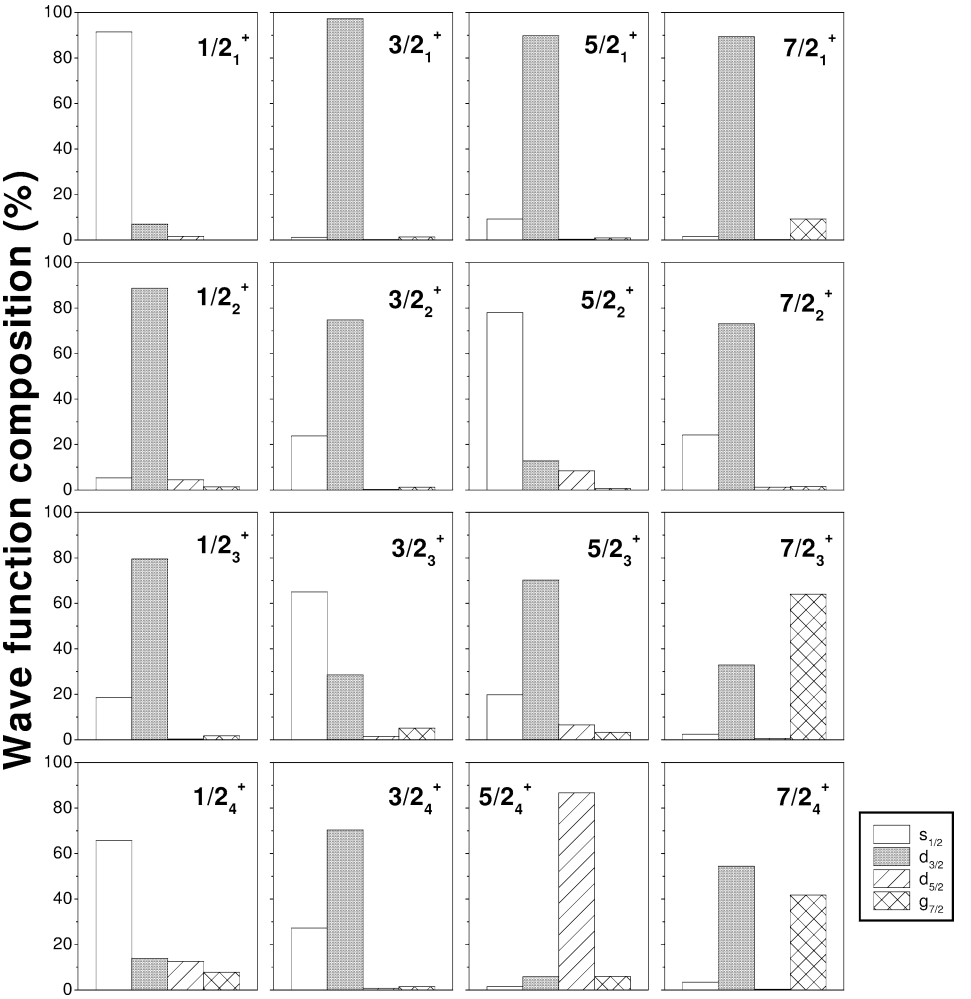

Fig. 6. The composition of the IBFM wavefunctions for the lowest levels of positive parity in ^{131}Te.

From Fig. 4 one can see that the positive parity states up to about 1.5 MeV excitation are reasonably well accounted for by the calculations. One can therefore say that these states result essentially from the coupling of quasiparticles to the lowest, collective core states. Fig. 6 shows the composition of the wavefunctions of the lowest few levels of positive parity. They are all dominated either by the $s_{1/2}$ or the $d_{3/2}$ orbital, with the exception of the $7/2^+$ states which start having important $g_{7/2}$ components. The mixing between these orbitals is not so important.

At higher energies, around 2 MeV, it becomes increasingly difficult to establish unambiguous connections between the experimental and calculated states. This is due both to ambiguities in the experimental spin and parity values, but also to the fact that the

number of calculated levels becomes too low, which already indicates that other excitation mechanisms may be present.

In the case of the negative parity values, the levels up to about 1.7 MeV excitation can also be put rather unambiguously in correspondence with calculated levels. All the calculated levels up to this energy have $h_{11/2}$ as main quasiparticle component. At higher excitation energies, especially above 2.0 MeV, it is very clear that the number of predicted states is much too low. This is especially the case for the many $3/2^-$ states, evidenced both in (n, γ) and in the (d, p) reaction. The IBFM fails to predict the correct fragmentation of the $p_{3/2}$ strength.

Some of these difficulties may have been anticipated as due to the too serious truncation offered by the IBM parametrization of the core. We would expect that this 'inert' core breaks above 2.0 MeV excitation, thus offering new excitation modes, which are not considered by the simple approach of the IBFM. For this reason, a comparison with the QPM, which has not such limitations, is worthwhile.

5.2. The quasiparticle–phonon model calculations

To study the properties of the ground and excited states in ^{131}Te within the QPM, the model Hamiltonian has been diagonalized for each j^π in a configuration space which contains quasiparticle qp, quasiparticle – 1 phonon $[qp \otimes 1ph]_{j^\pi}$, and quasiparticle – 2 phonon $[qp \otimes 2ph]_{j^\pi}$ configurations. Matrix elements of interactions between different configurations have been calculated making use of the model Hamiltonian and the internal fermion structure of the phonons. In the first order, only configurations which are different by one in the number of phonons have nonzero matrix elements of interaction. Configurations qp and $[qp \otimes 2ph]_{j^\pi}$; $[qp \otimes Nph]_{j^\pi}$ and other $[qp \otimes Nph]_{j^\pi}$ interact only in the second order, matrix elements of their interaction are smaller by few orders of magnitude as compared to the ones between $[qp \otimes Nph]_{j^\pi}$ and $[qp \otimes (N \pm 1)ph]_{j^\pi}$ and are neglected in the present calculations. In performing calculations, $[qp \otimes 1ph]_{j^\pi}$ and $[qp \otimes 2ph]_{j^\pi}$ configurations which violate the Pauli principle have been excluded from the configuration space according to an approximate procedure described in [36]. We refer to [36–38] for a more detailed description of the QPM application to odd-mass nuclei.

In the actual calculations, we have used the Woods–Saxon potential for the mean field with parameters for $A = 127$ from [39]. All single particle levels for protons and neutrons from $1s_{1/2}$ up to narrow quasi-bound states in the continuum have been accounted for. The strength parameter for monopole pairing for protons and neutrons is taken also from [39]. The phonon spectrum in the even–even core ^{130}Te has been obtained from solving the quasiparticle-RPA equation. Strength parameters of the residual interaction have been adjusted to reproduce the experimental B(E2) and B(E3) values for the lowest 2^+ and 3^- states in ^{130}Te, respectively. We have used a deduction of the mean field as a form factor of the QPM separable forces of the residual interaction and this allows us to employ the same strength parameters for other multipolaries with positive (negative) parity as for $J^\pi = 2^+$ ($J^\pi = 3^-$). In total, our phonon basis includes natural parity phonons with J^π from 0^+ to 7^- of different collectivity, from rather collective 2^+_1 and 3^-_1 to practically pure two-quasiparticle configurations.

After the phonon basis in the even–even core was fixed, the calculations of the spectra in ^{131}Te have been performed without any additional free parameters. To make calculations possible, the configuration space in ^{131}Te has been truncated and only all $[qp \otimes 1ph]_{j^\pi}$ below 6.5 MeV and all $[qp \otimes 2ph]_{j^\pi}$ below 7.5 MeV have been accounted for. The excitation energy of the 2_1^+ state in ^{130}Te equals 839 keV. So, in ^{131}Te, we expect the lowest $[qp \otimes 3ph]_{j^\pi}$ configuration around 2.5 MeV and the lowest $[qp \otimes 4ph]_{j^\pi}$ one around 3.4 MeV. Thus, although the configuration space contains several hundred states for each j^π in the present calculations, it is not complete and the fragmentation even of simple qp configurations should be somewhat underestimated.

To test the results of the QPM calculation we have compared them with experimental data obtained in this work. Like in the case of the IBFM we have used the level positions, the electromagnetic decay properties and the neutron transfer spectroscopic factors for this comparison. In addition to these quantities, very rich experimental data for negative

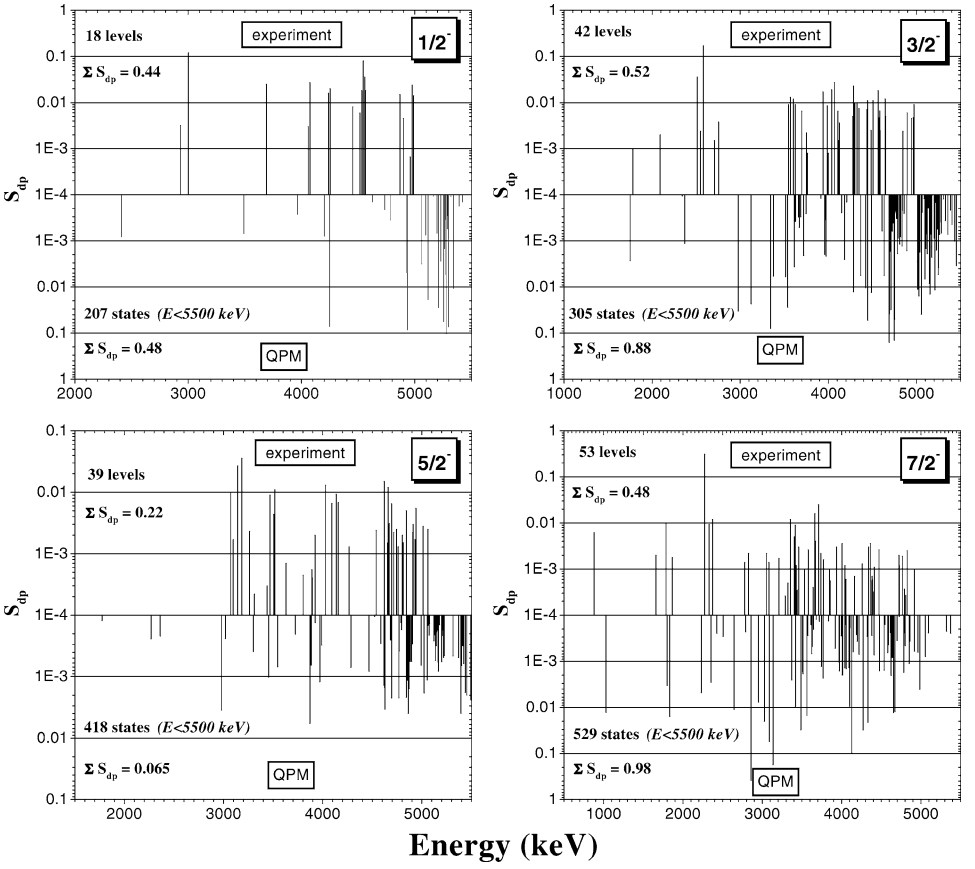

Fig. 7. The comparison of experimental distribution of $3p_{1/2}$, $3p_{3/2}$, $2f_{5/2}$ and $2f_{7/2}$ strengths with the QPM calculations.

parity states enable us to check predicted fragmentation of $3p_{1/2}$, $3p_{3/2}$, $2f_{5/2}$ and $2f_{7/2}$ strengths.

Examining Fig. 4 one can see essentially good correspondence of experimental and calculated level energies up to 1.8 MeV. Spin and parity ambiguities for some experimental levels prevent us to extend this one-to-one correspondence above this excitation energy. The correspondence given in Fig. 4 is well supported by the comparison of branching ratios for these levels (see Table 5) as well as by the well reproduced neutron transfer spectroscopic factors (see Fig. 5). Spectroscopic factors of the (d, p) reaction for J^π_ν states are defined in model calculations as

$$S_{dp}\left(J^\pi_\nu\right) = u^2_{J^\pi} C^2_\nu\left(J^\pi\right), \tag{3}$$

where u_{J^π} is the coefficient of the Bogoliubov transformation from particles to quasiparticles (i.e., $u^2_{J^\pi}$ is the "free phase space" for a stripping reaction) and $C^2_\nu(J^\pi)$ is a contribution of the quasiparticle configuration to the wave function of this state.

The experimental and calculated fragmentation is shown in Fig. 7. A qualitatively good agreement was obtained for the fragmentation of the lowest-lying single-particle strength $2f_{7/2}$. The calculated distribution of strengths for the other negative parity states is shifted into higher excitation energies. While in case $3/2^-$ this shift is relatively very small, several hundred keV, it is well pronounced for $1/2^-$ and $5/2^-$ strengths.

The lack of $1/2^-$ and $5/2^-$ states with relatively large spectroscopic factors below 5.2 MeV in the present QPM calculations as compared to the data may indicate that $l * s$ splitting in the Woods–Saxon potential used for the mean field is somewhat overestimated. Another possible explanation may be related to basis truncation. Although the employed basis is rather large, it is not complete as discussed above. In our Woods–Saxon potential we have the following quasiparticle energies: $7/2^-_\nu \Rightarrow 2.89$ MeV, $3/2^-_\nu \Rightarrow 4.28$ MeV,

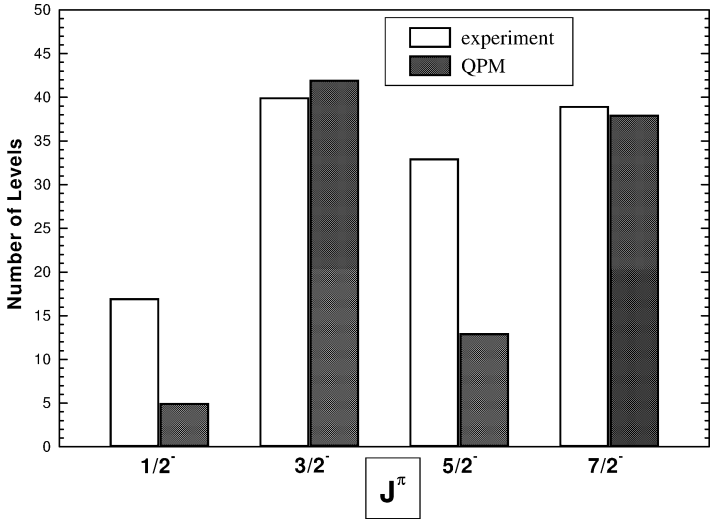

Fig. 8. The comparison of numbers of observed $1/2^-$, $3/2^-$, $5/2^-$ and $7/2^-$ levels with the QPM calculations. Both sets of numbers include states below excitation energy $E < 5.2$ MeV and with $S_{dp} \geqslant 10^{-3}$.

$1/2^-_\nu \Rightarrow 5.07$ MeV, and $5/2^-_\nu \Rightarrow 5.97$ MeV. It is clear that fragmentation of the last two of them suffers mostly from neglecting of $[qp \otimes 1ph]$ configurations above 6.5 MeV. Our test with an increase of this maximum energy from 5.5 to 6.5 MeV demonstrates sufficient improvement in agreement with the data for $1/2^-$ and $5/2^-$ states.

To compare the experimental and calculated fragmentation quantitatively we have selected energy and strength regions within which both the experiment and the theory could give reasonably complete information. In Fig. 8 numbers of levels up to 5.2 MeV and with one-neutron transfer spectroscopic strength $S_{dp} \geqslant 10^{-3}$ predicted by the QPM calculation are compared with the experimental data. The very good agreement for $3/2^-$ and $7/2^-$ contrasts with the failure of the QPM prediction for $1/2^-$ and $5/2^-$.

6. The determination of the thermal neutron cross section

Besides the value of the thermal neutron capture recommended in the BNL neutron cross section atlas [40], $\sigma_{n\gamma}^{g+m} = 290$ mb, other values were reported in the wide range from 161 to 310 mb [41–44]. The intensities of γ-rays following the thermal neutron capture in ^{130}Te were used in the work by Honzátko et al. [14]. Combining the absolute normalization via β-decay and the measurement with composite Te–Al and Te–KCl targets the total capture cross section was determined to be $\sigma_{n\gamma}^{g+m} = 193 \pm 20$ mb. In the present work we used a similar approach. To calculate the total thermal neutron capture cross section we used the intensities of the three strongest γ lines I_γ and the partial elemental cross sections $\sigma_{n\gamma}^{\text{elem}}$ from a preliminary measurement in Budapest with a natural Te target [45]

$$\sigma_{n\gamma} = \frac{\sigma_{n\gamma}^{\text{elem}}}{\text{Abundance}_{130} \times I_\gamma}. \tag{4}$$

The results of this calculation are summarized in the Table 6.

The weighted average value $\sigma_{n\gamma}^{g+m} = 186 \pm 13$ mb is in perfect agreement with the work by Honzátko et al. [14]. The weighted average of thermal neutron capture cross section from above mentioned works [41–44] is $\sigma_{n\gamma}^{g+m} = 200 \pm 20$ mb. On the other hand our value is about 1.5 times smaller than value adopted in the BNL compilation [40] of $\sigma_{n\gamma}^{g+m} = 290 \pm 70$ mb.

Table 6
Determination of the thermal neutron capture cross section

E_γ (keV)	Int. (%)	$\sigma_{n\gamma}^{\text{elem}}$ (mb) [45]	$\sigma_{n\gamma}$ (mb)
296.0	47.66(39)	29(3)	180(19)
2286.5	26.77(29)	18(2)	196(23)
3346.8	32.00(21)	20(3)	185(28)
Mean			186(13)

7. Direct mechanism in (n, γ) reaction

Despite the application of slow neutron capture since long time long in nuclear spectroscopy some gaps still exist in the knowledge of the reaction mechanism itself. For most of the isotopes the thermal neutron capture is considered to go via a compound nucleus resulting in the statistical character of this reaction. Nevertheless, there are places in the table of isotopes, especially around closed shells, where direct capture was observed. The first expression for the calculation of the partial direct cross section of E1 transitions in slow neutron capture were derived by Lane and Lynn [46]. The commonly used formula for a even–even target is given in the atlas of neutron cross section [40]

$$\sigma_{\gamma f}(\text{channel}) = \sigma_{\gamma f}(\text{hard sphere})\left[1 + \frac{R - a_{\text{coh}}}{R} Y_f \frac{Y_f + 2}{Y_f + 3}\right]^2, \tag{5}$$

where

$$\sigma_{\gamma f}(\text{hard sphere}) = \frac{0.062}{R\sqrt{E_n}}\left[\frac{Z}{A}\right]\frac{2J_f + 1}{6(2J_t + 1)} S_{dp} Y_f^2 \left[\frac{Y_f + 3}{Y_f + 1}\right]^2 \tag{6}$$

and

$$Y_f^2 = \frac{2mE_\gamma R^2}{\hbar^2}. \tag{7}$$

Z is the proton number, A is the atomic number, R is the interaction radius (usually taken in the form $1.35 \times A^{1/3}$ fm), a_{coh} is the coherent scattering length, J_f is the total spin of final state, J_t is the spin of the target, S_{dp} is the (d, p) spectroscopic factor, E_γ is the energy of the primary γ transition and E_n is the incident neutron energy (0.0253 eV for 2200 m/s neutrons).

The studied isotope ^{131}Te is very suitable for the investigation of the direct mechanism in thermal neutron capture. The first evidence for the presence of direct neutron capture in this isotope was published more than 20 years ago [13]. This evidence was based on the four strongest primary E1 γ transitions in the (n_{th}, γ) reaction.

The present study enables us to investigate this mechanism in more details. We observed 40 states which were populated by primary E1 transitions in the (n_{th}, γ) reaction as well as in the (d, p) reaction with a $l = 1$ transfer. These states cover a wide range of excitation energies from 2.2 MeV up to 5 MeV and also more than two orders of magnitude of the intensity of the primary γ transitions. Using the simple formula Eq. (5) we compared the experimental partial thermal neutron capture cross sections for these states with theoretical predictions. The result of this comparison is shown in Fig. 9. From this figure one can see a very strong correlation between the experimental data and the calculation. On the other hand, the calculated values are 3.3 times smaller than experimental ones.

The high correlation can be documented quantitatively by the correlation coefficient between the experimental and calculated direct partial cross sections being $\rho = 0.99$. Thus, we can conclude that the direct process is very dominantly responsible for the primary population of these levels. The total primary intensity feeding these levels accounts for about 90% of the thermal neutron capture cross section.

We have observed the three primary γ transitions to levels with $5/2^+$ spin. With respect to the spin of the capture state, $1/2^+$, these transitions are supposed to have an E2

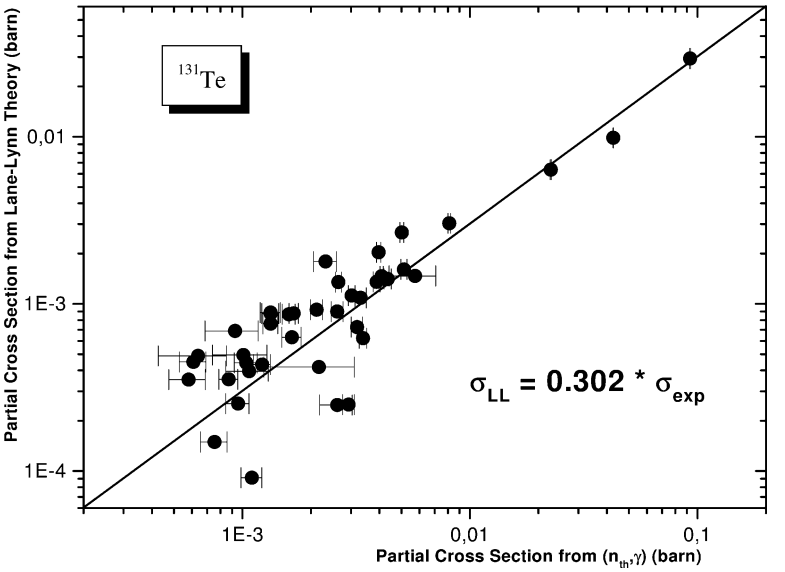

Fig. 9. The comparison of the experimental partial cross section from the $(n_{\mathrm{th}}, \gamma)$ with theoretical prediction from the Lane–Lynn model of direct capture, see for instance [40].

character. The very dominant direct E1 capture together with the very small contribution from positive resonances into the thermal neutron capture, ≈ 1 mb [40], leads us to test the possibility of direct E2 capture character of these transitions. To calculate the direct E2 contribution for these levels we have used the formula derived in Ref. [47]

$$\sigma_{n\gamma}^{DC} = \frac{1}{4\pi\varepsilon_0}\frac{(2J_f+1)S_{dp}}{2(2J_t+1)}\frac{\pi\bar{e}^2}{300\hbar v_n}\left(\frac{A+1}{A}\right)^5 \frac{\lambda\!\!\!^{-5}_c}{R^3} \times Y_f^6\left[\frac{Y_f^2+7Y_f+15}{Y_f^2+3Y_f+3}+\frac{Y_f}{R}(R'-a_{\mathrm{coh}})\frac{Y_f^2+5Y_f+8}{Y_f^2+3Y_f+3}\right]^2, \tag{8}$$

where J_f,J_t, A, R, a_{coh}, S_{dp} and Y_f have the same meaning as in Eqs. (5) and (6) and v_n is the velocity of the neutron, R' is the potential scattering length, $\bar{e}$ is the E2 effective neutron charge and $\lambda\!\!\!^{-}_c$ is the Compton wavelength of the neutron. Introducing the E2 effective neutron charge factor $\xi = \bar{e}/e$ we evaluated the direct capture contribution for the three levels populated with the primary E2 transitions. The calculated values of the direct E2 contributions and the experimental values of the partial cross sections are given in Table 7. Assuming $\xi \approx 0.5$ [47,48], the calculated direct E2 contributions are too small to explain the intensities of these primary E2 transitions. Nevertheless, these primary E2 transitions deserve more detailed investigations.

Table 7
The observed E2 primary transitions

E_γ (keV)	Int. (%)	$\sigma_{n\gamma}^{\exp}$ (mb)	E_f (keV)	$(2J_f+1)S_{dp}$	$\sigma_{n\gamma}^{DC}/\xi^2$ (mb)
4721.9	0.12(5)	0.22	1207.1	0.16	0.036
4207.4	0.39(4)	0.73	1721.6	0.02	0.003
3912.7	0.54(14)	1.00	2015.4	0.03	0.004

8. Conclusions

The present work is a part of our systematic investigation of Te isotopes. It is a detailed study of ^{131}Te the heaviest Te isotope from this investigated chain. Complementary methods of nuclear spectroscopy, (n,γ) and (d,p), supplied the experimental data for the construction of an extensive level and decay scheme as well as for the study of the nuclear structure of ^{131}Te. About 290 levels were identified within the excitation energy range up to 5.2 MeV. More than 400 γ transitions out of 438 totally observed were placed into the decay scheme of ^{131}Te. Properties of low-lying states up to 2.5 MeV were compared with theoretical predictions made by IBFM and QPM models.

The IBFM calculation describes excitation energies, electromagnetic properties and spectroscopic strength of low-lying states rather well using parameters smoothly extrapolated from those of the lighter Te isotopes [2]. The 'boson cut-off' effect become evident at higher excitation energies.

Like the IBFM calculations, the QPM results were tested using the nuclear properties of low-lying states. With the QPM model we are able to reproduce excitation energies, electromagnetic properties and (d,p) spectroscopic strengths up to 1.8 MeV. In addition to the comparison of nuclear properties of low-lying states, we have compared the experimental fragmentation of $3p_{1/2}$, $3p_{3/2}$, $2f_{5/2}$ and $2f_{7/2}$ strengths with the QPM prediction. The comparisons for these four fragmentations indicate that the $l*s$ splitting used in the QPM calculation is somewhat overestimated.

We determined also the isomeric ratio of the $11/2^-$ isomer, the neutron binding energy and the thermal neutron capture cross section of ^{130}Te, and investigated the direct mechanism in thermal neutron capture.

Acknowledgements

This work was supported by the Grant Agency of the Czech Republic (No. 202/99/k038) and (No. 202/99/D087) and by the DFG under contract FOR 272/2-1. We wish to thank N. Pietralla, P. von Brentano, H. Machner and G. Bohlen for target material, P. Maier-Komor and K. Nacke for target preparation and Th. Faestermann for Q3D maintenance. We would like to thank G. Molnar and R. Firestone for fruitful discussions and preliminary (n,γ) data with a natural tellurium target in Budapest.

References

[1] D. Bucurescu, T. von Egidy, H.-F. Wirth, N. Marginean, U. Köster, G. Graw, A. Metz, R. Hertenberger, Y. Eisermann, Nucl. Phys. A 674 (2000) 11.
[2] D. Bucurescu, T. von Egidy, H.-F. Wirth, N. Marginean, W. Schauer, I. Tomandl, G. Graw, A. Metz, R. Hertenberger, Y. Eisermann, Nucl. Phys. A 672 (2000) 21.
[3] W. Schauer, C. Doll, T. von Egidy, R. Georgii, J. Ott, H.-F. Wirth, A. Gollwitzer, G. Graw, R. Hertenberger, B. Valnion, M. Grinberg, Ch. Stoyanov, Nucl. Phys. A 652 (1999) 339.
[4] V. Bondarenko, T. von Egidy, J. Honzátko, I. Tomandl, D. Bucurescu, M. Marginean, J. Ott, W. Schauer, H.-F. Wirth, C. Doll, Nucl. Phys. A 673 (2000) 85.
[5] R. Georgii, T. von Egidy, J. Klora, H. Lindner, U. Mayerhofer, J. Ott, W. Schauer, P. von Neumann-Cosel, A. Richter, C. Schlegel, R. Schulz, V.A. Khitrov, A.M. Sukhovoj, A.V. Vojnov, J. Berzins, V. Bondarenko, P. Prokofjevs, L.J. Simonova, M. Grinberg, Ch. Stoyanov, Nucl. Phys. A 592 (1995) 307.
[6] C. Doll, H. Lehmann, H.G. Börner, T. von Egidy, Nucl. Phys. A 672 (2000) 3.
[7] J. Honzátko, I. Tomandl, V. Bondarenko, D. Bucurescu, T. von Egidy, J. Ott, W. Schauer, H.-F. Wirth, C. Doll, A. Gollwitzer, G. Graw, R. Hertenberger, B. Valnion, Nucl. Phys. A 645 (1999) 331.
[8] J. Ott, C. Doll, T. von Egidy, R. Georgii, M. Grinberg, W. Schauer, R. Schwengner, H.-F. Wirth, Nucl. Phys. A 625 (1997) 598.
[9] V. Bondarenko, T. von Egidy, H.-F. Wirth, A. Metz, Y. Eisermann, G. Graw, R. Hertenberger, L. Rubaček, Jahresbericht, Beschleunigerlaboratorium der Universität und Technischen Universität München, 1998, p. 18.
[10] H.-F. Wirth, T. von Egidy, C. Doll, U. Köster, W. Schauer, I. Tomandl, J. Honzátko, V. Bondarenko, D. Bucurescu, G. Graw, Y. Eisermann, R. Hertenberger, A. Metz, in: S. Wender (Ed.), Proceedings Capture Gamma-Ray Spectroscopy and Related Topics, in: AIP Conference Proceedings, Vol. 529, 2000, p. 663.
[11] Yu.V. Segeenkov, Yu.L. Khazov, T.W. Burrows, M.R. Bhat, Nucl. Data Sheets 72 (1994) 487.
[12] E.A. Rudak, A.V. Soroka, V.N. Tadeush, in: 27th Soviet Conference on Nuclear Structure, Taskhent, 1977, p. 60.
[13] J. Honzátko, K. Konečný, F. Bečvář, E.A. Eissa, Czech. J. Phys. B 30 (1980) 763.
[14] J. Honzátko, K. Konečný, Z. Kosina, F. Bečvář, E.A. Eissa, Czech. J. Phys. B 34 (1984) 520.
[15] R.K. Jolly, Phys. Rev. 136 (1964) B683.
[16] A. Graue, E. Jestad, J.R. Lien, P. Torvund, W.H. Moore, Nucl. Phys. A 103 (1967) 209.
[17] A. Strömich, B. Steinmetz, R. Bangert, B. Gonsior, M. Roth, P. von Brentano, Phys. Rev. C 16 (1977) 2193.
[18] M.A.M. Shahabuddin, J.A. Kuehner, A.A. Pilt, Phys. Rev. C 23 (1981) 64.
[19] J. Blachot, H.N. Erten, C.D. Coryell, E.S. Macias, W.B. Walters, Phys. Rev. C 4 (1971) 214.
[20] V. Hnatowicz, J. Kristak, M. Fiser, D. Venos, J. Jursik, Czech. J. Phys. 25B (1975) 1.
[21] M. Löffler, H.J. Scheerer, H. Vonach, Nucl. Instrum. Methods 111 (1973) 1.
[22] E. Zanotti, M. Bisenberger, R. Hertenberger, H. Kader, G. Graw, Nucl. Instrum. Methods A 310 (1991) 706.
[23] P.D. Kunz, Computer Code CHUCK3, University of Colorado, unpublished.
[24] P.R. Christensen, G. Lovhoiden, J. Rasmussen, Nucl. Phys. A 149 (1970) 302.
[25] G.A. Lalazissis, S. Raman, P. Ring, At. Data Nucl. Data Tables 71 (1999) 1.
[26] J. Honzátko, K. Konečný, I. Tomandl, J. Vacík, F. Bečář, P. Cejnar, Nucl. Instrum. Methods A 376 (1996) 434.
[27] B. Krusche, K.P. Lieb, H. Daniel, T. von Egidy, G. Barreau, H.G. Börner, R. Brissot, C. Hofmeyr, R. Rascher, Nucl. Phys. A 386 (1982) 245.
[28] V. Bondarenko, J. Honzátko, I. Tomandl, D. Bucurescu, T. von Egidy, J. Ott, W. Schauer, H.-F. Wirth, C. Doll, Phys. Rev. C 60 (1999) 027302.
[29] K. Schreckenbach, Program LEVFIT, ILL Grenoble, 1975.
[30] G. Audi, A.H. Wapstra, Nucl. Phys. A 565 (1993) 66.
[31] F. Iachello, O. Scholten, Phys. Rev. Lett. 43 (1979) 679.
[32] V.G. Soloviev, Theory of Atomic Nuclei: Quasiparticles and Phonons, Institute of Physics, Bristol, 1992.
[33] Yu.V. Sergeenkov, Nucl. Data Sheets 65 (1992) 277.
[34] O. Scholten, Computer code SPEC, unpublished.
[35] O. Scholten, T. Ozzello, Nucl. Phys. A 424 (1984) 221.
[36] A.I. Vdovin, V.V. Voronov, V.G. Soloviev, Ch. Stoyanov, Sov. J. Part. Nucl. 16 (1985) 105.

[37] S. Gales, Ch. Stoyanov, A.I. Vdovin, Phys. Rep. 166 (1988) 125.
[38] J. Bryssinck, L. Govor, V.Y. Ponomarev, F. Bauwens, O. Beck, D. Belic, P. von Brentano, D. De Frenne, C. Fransen, R.-D. Herzberg, E. Jacobs, U. Kneissl, H. Maser, A. Nord, N. Pietralla, H.H. Pitz, V. Werner, Phys. Rev. C 62 (2000) 014309.
[39] A.I. Vdovin, V.V. Voronov, V.Y. Ponomarev, Ch. Stoyanov, Sov. J. Nucl. Phys. 30 (1979) 479.
[40] S.F. Mughbahab, M. Divideenam, N.E. Holden (Eds.), Neutron Cross Section, Vol. 1, Part A, Academic Press, 1981, p. 12.
[41] L. Seren, H.N. Friedlander, S.H. Turkel, Phys. Rev. 72 (1947) 888.
[42] S.K. Mangal, P.S. Gill, Nucl. Phys. 36 (1962) 542.
[43] M.L. Sehgal, Phys. Rev. 128 (1962) 761.
[44] M.D. Ricabarra, R. Turjanski, G.H. Ricabarra, C.B. Bigham, Can. J. Phys. 46 (1968) 2473.
[45] G. Molnar, T. Belgya, R.B. Firestone, private communication, 2001.
[46] A.M. Lane, J.E. Lynn, Nucl. Phys. 17 (1960) 63;
A.M. Lane, J.E. Lynn, Nucl. Phys. 17 (1960) 686.
[47] W.V. Prestwich, T.J. Kennet, Phys. Rev. C 30 (1984) 392.
[48] B. Castel, Y.K. Ho, Phys. Rev. C 34 (1986) 408.